

# Consequences of Measuring Stellar Positions at the 50 Microarcsecond Level

Marc A. Murison

U. S. Naval Observatory  
Washington, DC

February 26, 2001

This presentation is available at <http://aa.usno.navy.mil/murison/talks/>

# Abstract

---

The Full Sky Astrometric Mapping Explorer (FAME) is a NASA MIDEX mission (launch in late 2004) that will perform an all-sky astrometric and photometric survey with unprecedented accuracy of 40 million stars between 5th and 15th magnitude. FAME is unique in that solar radiation pressure drives the scanning pattern and attitude control. The level of measurement sensitivity and the unusual spacecraft configuration lead to many interesting consequences in both astrophysics and the spacecraft dynamics. This talk will present a brief overview of the astrophysics that FAME will address, then it will touch upon a few of the fascinating dynamical problems one must consider with an orbiting, quarter of a nanoradian instrument under passive control.

NOTE: This presentation is available at <http://aa.usno.navy.mil/murison/talks/>

# Theme for the Day

---

When dealing with tens of **microarcseconds** (i.e., tenths of **nanoradians**), all physical processes, no matter how insignificant in normal life, must be assumed significant until proven otherwise.

# Outline

---

- ▶ The FAME spacecraft and instrument
- ▶ Overview of astrophysics FAME will significantly impact
  - Calibration of the extragalactic distance scale
  - Stellar structure and evolution
  - Mass distribution of our Galaxy
  - Giant planet and brown dwarf detection
- ▶ A sampling of fun dynamics
  - Constraints on astrometric accuracies due to the observation scanning pattern
  - Consequences of solar irradiance fluctuations
  - Star image motions at the focal plane due to spacecraft dynamical perturbations

# Mission Comparison

---

	errors	Vmag	$\Delta T$ yr	stars	type	global?	cost
current ground	~a few mas	?	decades	hundreds	pointed	no	?
Hipparcos	1500 $\mu$ as	~9	2.5	118,000	survey	yes	800 M
FAME	30-500 $\mu$ as	5-15	2.5 -5	$40 \times 10^6$	survey	yes	140 M
Newcomb	10-20 $\mu$ as	14	2.5	a few $10^3$	pointed	yes	100 M
future ground	~10 $\mu$ as	~20	10-20	hundreds	pointed	no	100 M
POINTS	~1 $\mu$ as	18	5-10	$10^5$	pointed	yes	400 M
GAIA	4-200 $\mu$ as	5-20	5	$\sim 10^9$	survey	yes	>1-2 G?
SIM	~1 $\mu$ as	20?	5	$10^4$	pointed	yes	>2-3 G

# About FAME

---

- ▶ Primarily an **astrometric** instrument
- ▶ Measures positions, proper motions, and parallaxes of 40 million stars
  - to better than 50  $\mu\text{as}$  or  $\mu\text{as/yr}$  (0.24 nrad or nrad/yr) for stars brighter than 9th magnitude
  - to better than 500  $\mu\text{as}$  or  $\mu\text{as/yr}$  for stars brighter than 15th magnitude
- ▶ Photometry: four Sloan DSS bands, to millimagnitude accuracy
- ▶ Primary mission length: 2.5 years
  - Extended mission: 5 years
  - position & parallax errors scale as  $T^{-1/2}$
  - proper motion errors scale as  $T^{-3/2}$
- ▶ Instrument consists of
  - two telescopes, separated on the sky by 84 degrees. Both fields of view are routed to the same focal plane.
    - Apertures: 56 x 13 cm each.
    - focal length: 15 m
  - 24 CCD detectors (2048 x 4096 pixels each)
    - bandpass: 400-900 nm
    - 15 x 15 micron pixels

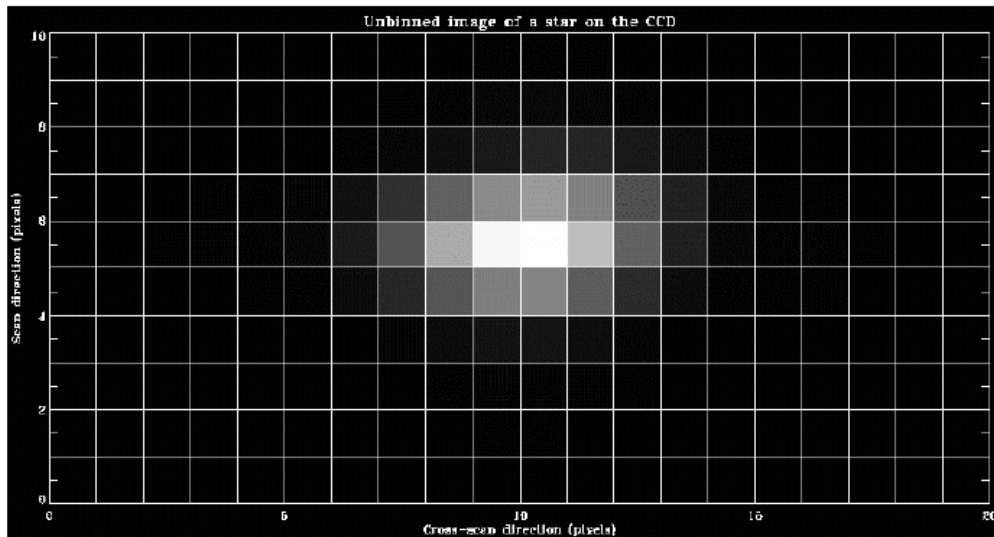
## About FAME (*continued*)

---

- ▶ Sky coverage follows from spin, precession, and Earth orbital motions.
- ▶ Spin period: 40 minutes
- ▶ Precession period: 20 days
- ▶ CCDs use time delay integration ("TDI mode")
  - CCD clock rate is synchronized with rate of motion of stars across the focal plane
  - Hence, the charge moves along with the stars for better S/N
- ▶ Nominal single-measurement precision:  
 $590 \mu\text{as} = 2.9 \text{ nrad} = 1/350 \text{ of a pixel}$
- ▶ Orbit: geosynchronous
  - Our orbit slot sits in a local minimum of the geopotential — no station keeping required!
- ▶ Precession of spin axis about nominal Sun direction is driven entirely by solar radiation pressure acting on the spacecraft Sun shield.
  - Very infrequent thruster firings
    - once per  $\sim 0.5$  (longer?) days
    - data reduction: need only several spin periods between firings for nearly maximal error suppression.

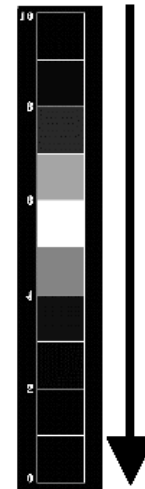
# On-board data processing

Unbinned image of a star on the CCD



On-chip  
binning

scan  
direction



scan  
direction

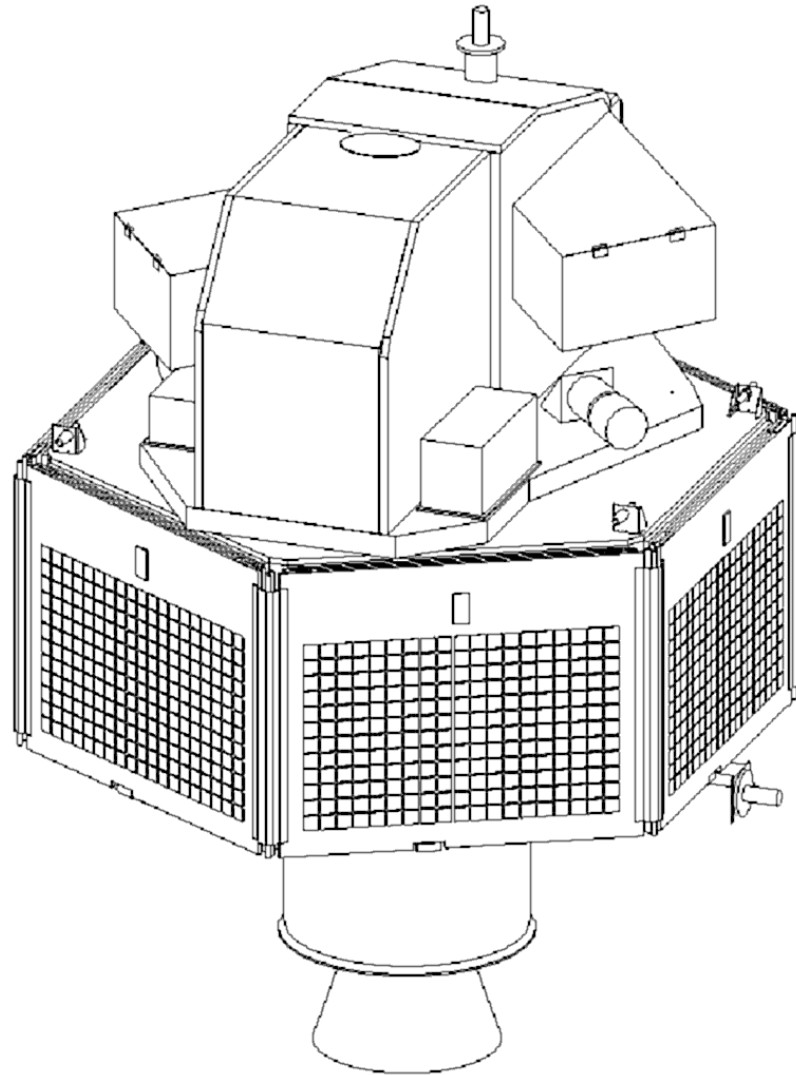
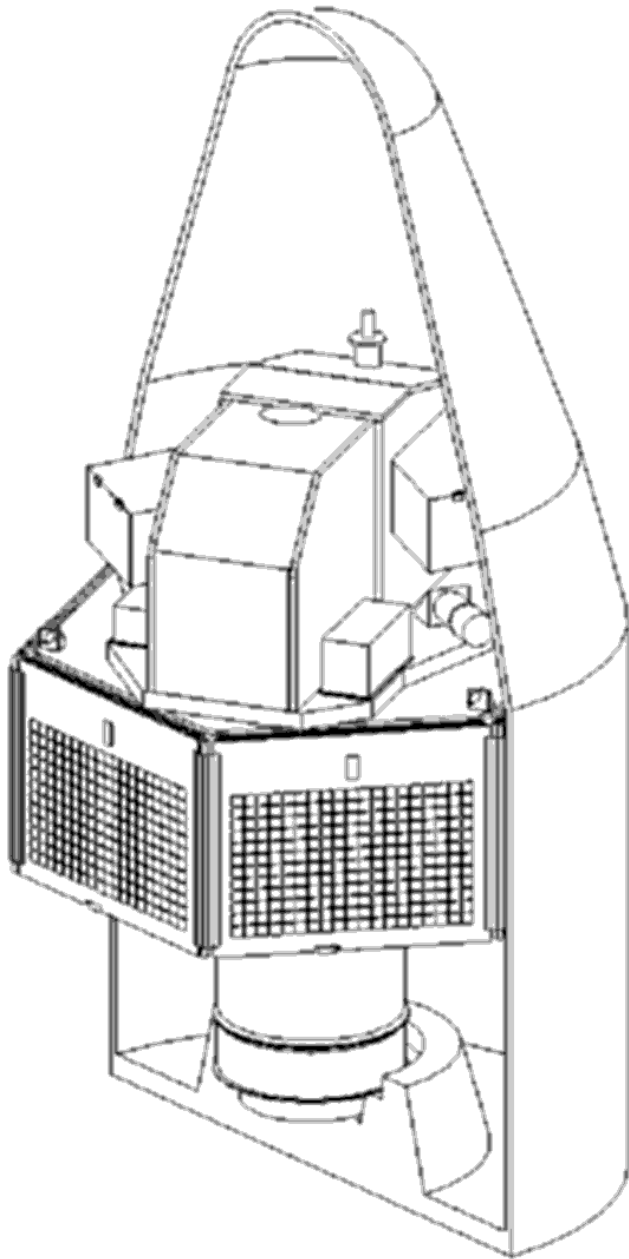
Pixels in the cross-scan direction

- ◆ The data from most stars are binned by 20 in the cross-scan direction on the CCD before being read-out



# Launch and GTO Configurations

---

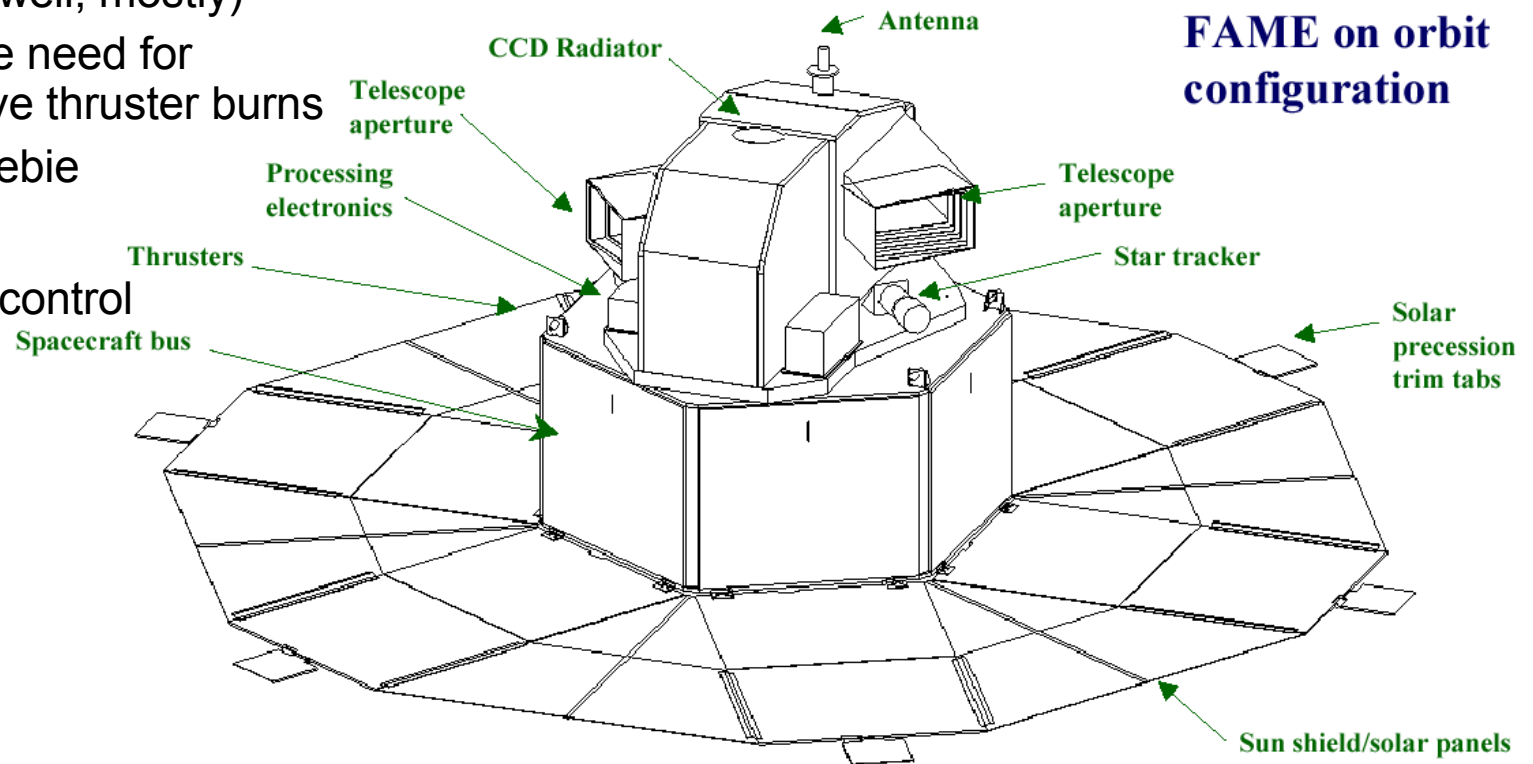


# Operational Configuration

- ▶ High degree of symmetry

- ▶ Solar shield

- thermal protection
- electrical power
- **precession torque**
  - steady (well, mostly)
  - very little need for corrective thruster burns
  - it's a freebie
- "trim tabs"
  - attitude control

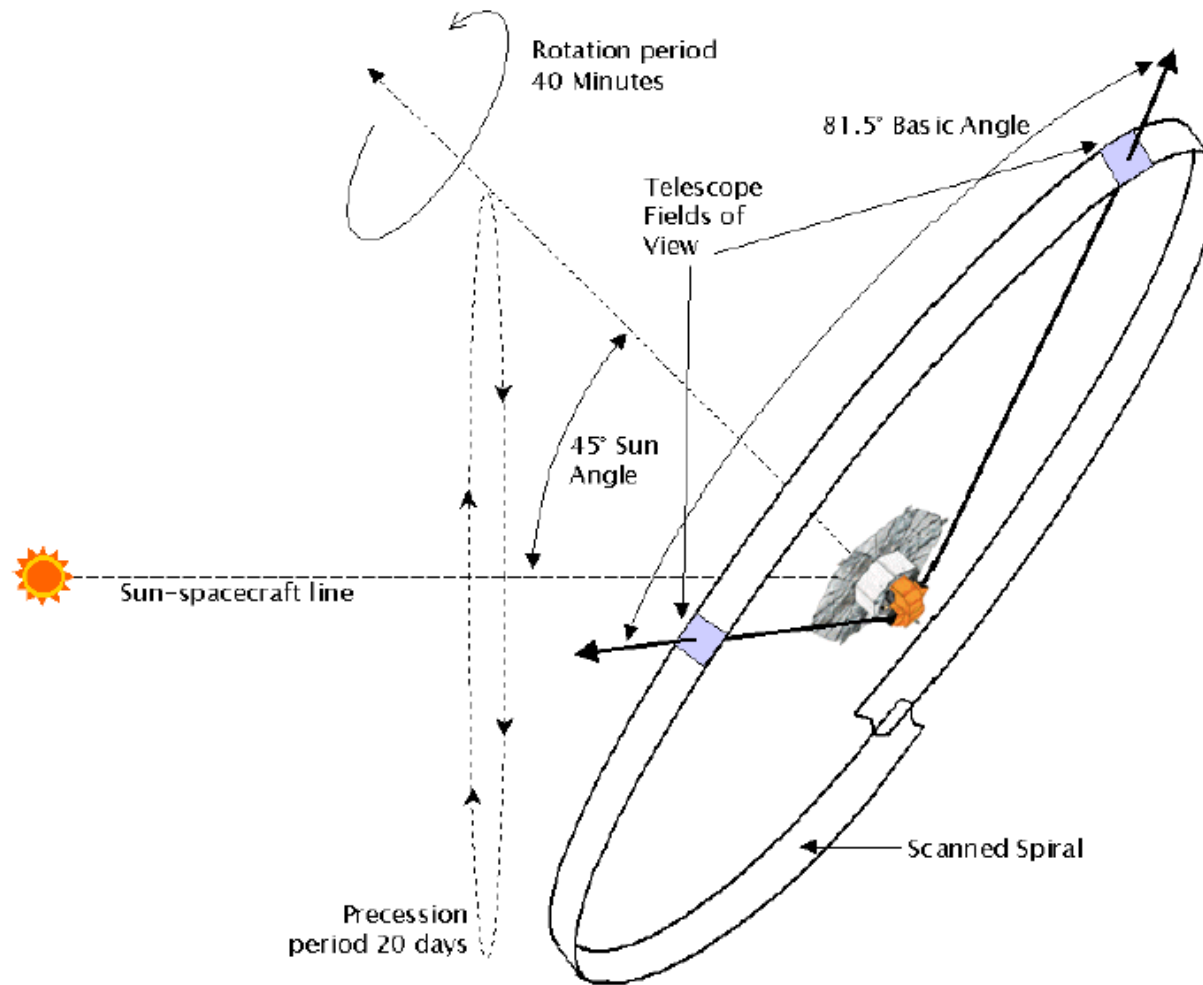


**FAME on orbit configuration**

**Spacecraft design uses component heritage from Clementine**

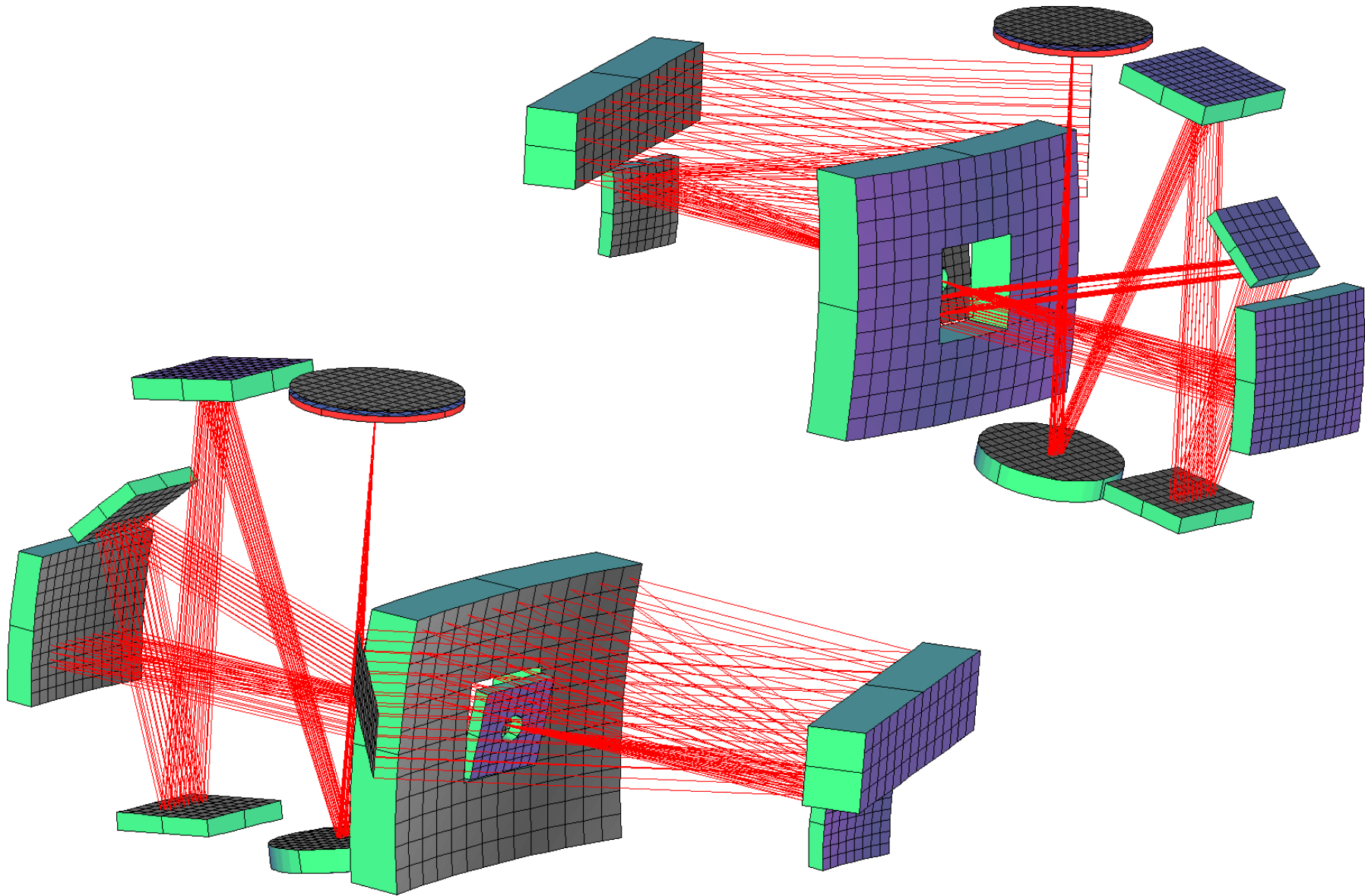
# Observational Mode

---



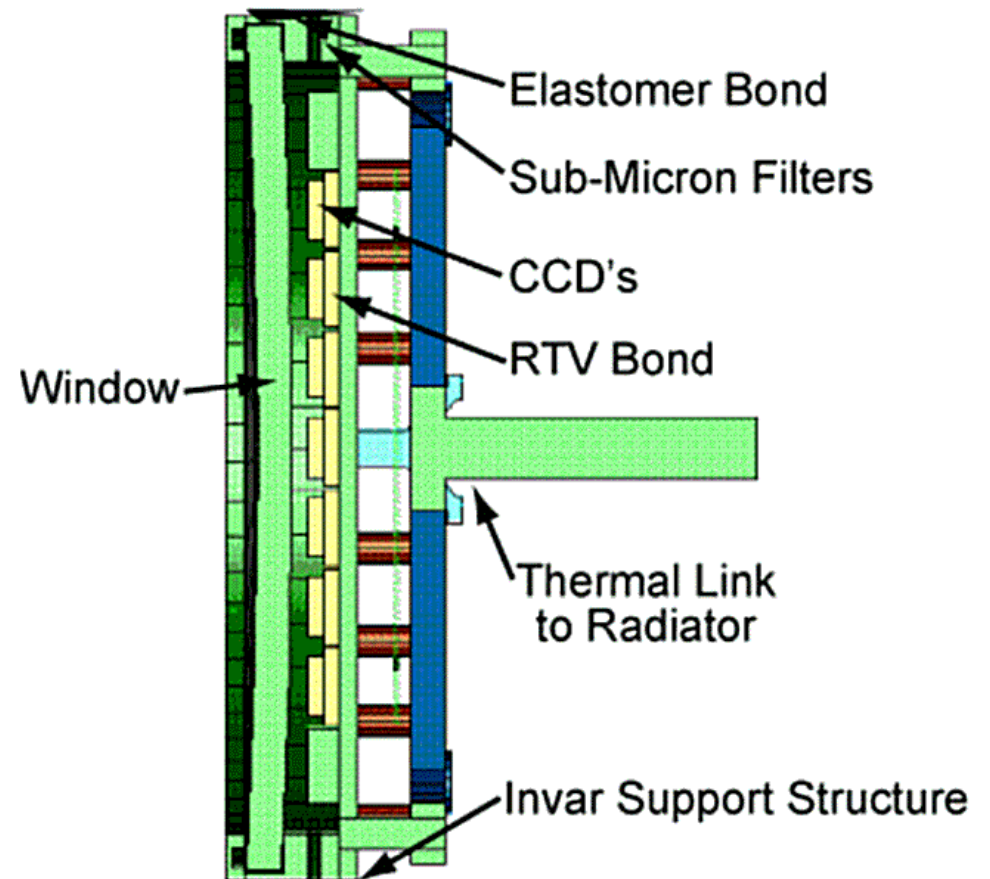
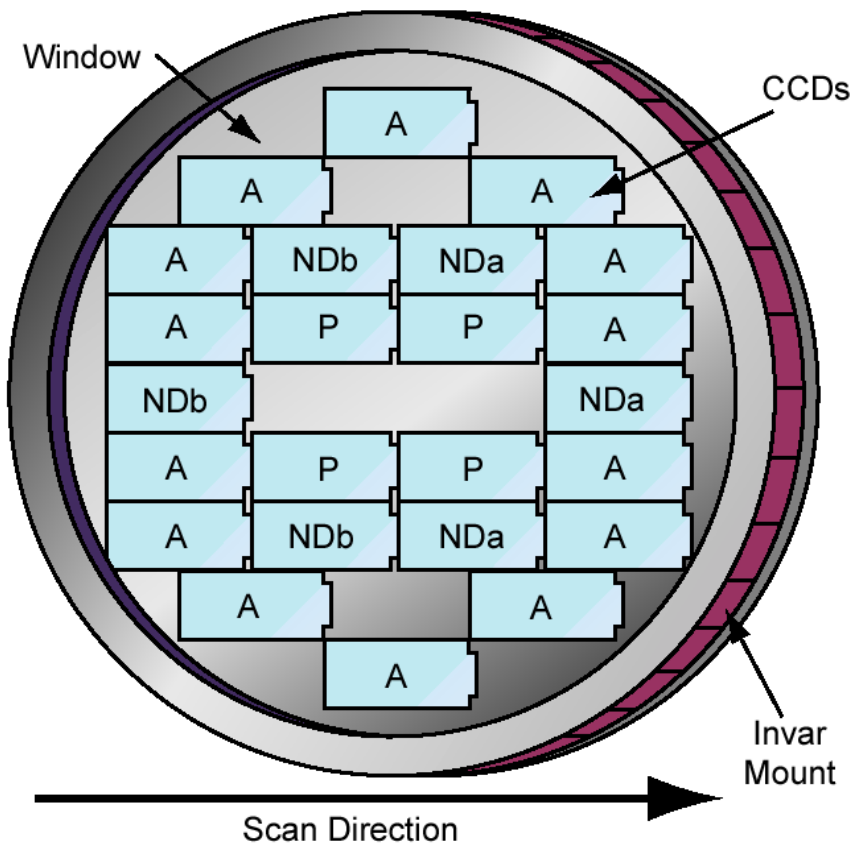
# Instrument Optical Layout

---



# Focal Plane Assembly

- ▶ 24 2048x4096 CCDs
- ▶ Thermal window



# Astrophysics



**FAME will calibrate the luminosities of stars for studies of stellar structure and evolution**

**FAME will detect non-linear proper motions, indicating binary, brown dwarf, and giant planet companions**

**2 kpc - distance within which the FAME error is <10%**  
• Contains >198 Cepheids  
• Contains >147 RR Lyrae stars

**0.1 kpc - distance within which the Hipparcos error is <10%**

**FAME will study the kinematic properties of stars in the galactic disk to determine the abundance of dark matter in the galactic disk**

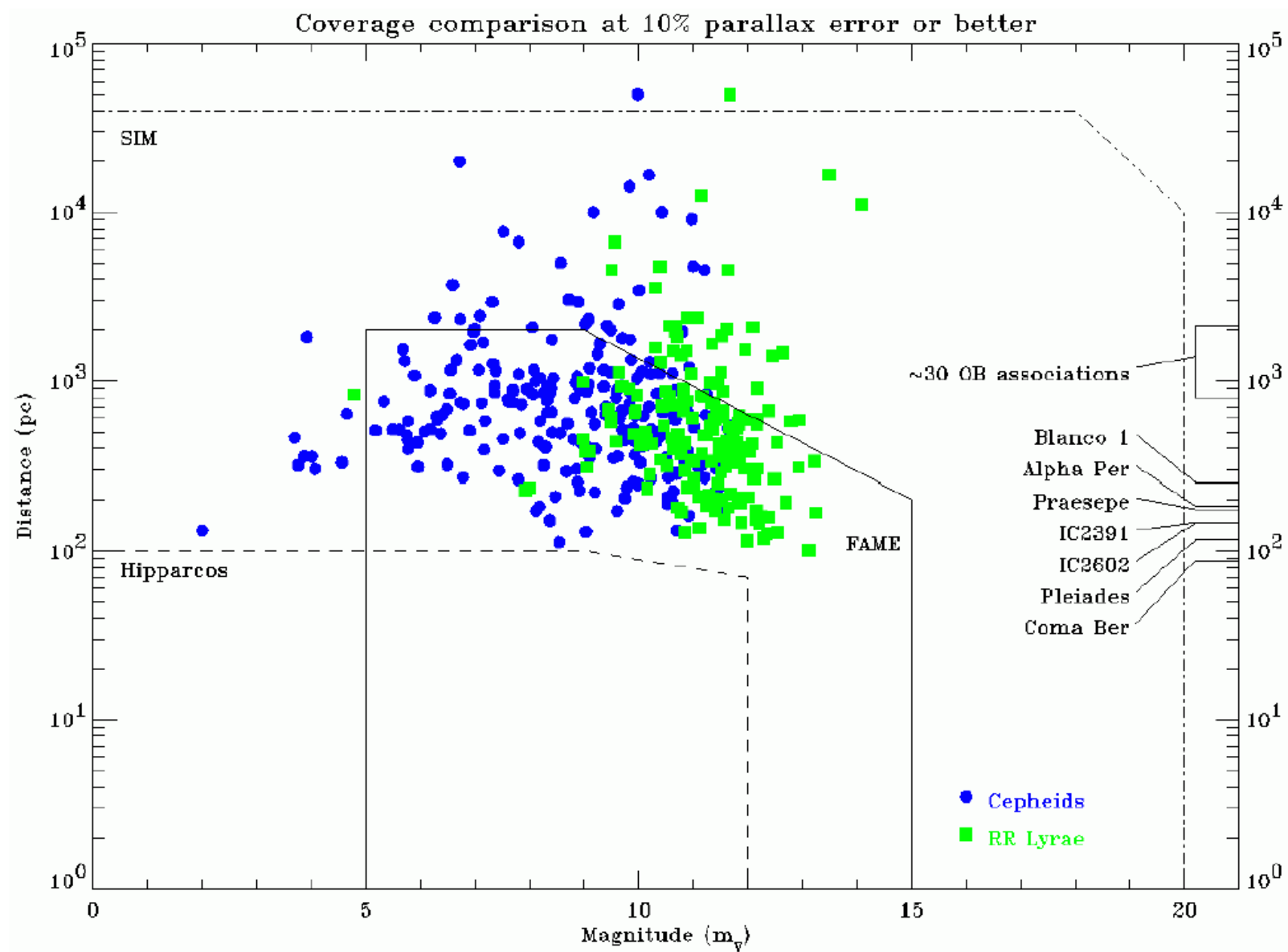
**FAME will calibrate the absolute luminosities of standard candle stars that are the foundation of the distance scale to other galaxies, including the Magellanic Clouds**

# FAME Science Highlights

---

- ▶ Serendipity
- ▶ Extragalactic Distance Scale
  - calibrate to  $\sim 1\%$  the Cepheid PLC relation (current  $\sim 10\%$ )
  - reddening a problem for all known Cepheids
    - parallax distances not affected by reddening
- ▶ Galactic Mass Distribution
  - distances & proper motions for stars of all spectral types
    - determine Oort A and B constants
    - distance scale for Galaxy
    - local Galactic rotation curve
    - local escape speed
    - local mass density
    - disk dark matter fraction





# FAME Science Highlights

---

## ► Galactic Structure

- Spiral arms: traveling density waves, or propagating star formation?
  - need 5% distance, 1% PM measurements of Perseus Arm (~2 kpc) peculiar motions
  - probably just out of reach of FAME capabilities
- rotation curve beyond Solar circle
- galactic thick disk component
  - need <10% distances to >2 kpc

## ► Globular Clusters

- FAME: direct distances and proper motions of 5 nearest (1.9 to 3.4 kpc)
- 50  $\mu\text{as/yr}$  at 2 kpc = 474 meters/sec !

## ► Open Clusters

- key to testing stellar evolution theory
- young clusters: tracers of star formation and spiral arms
- old clusters: important for Galactic disk evolution
- 19 old clusters with ages >1 Gyr lie within ~1.7 kpc
- need 5% distances
- FAME: distances to all eight clusters within 200 pc to better than 1%

# FAME Science Highlights

---

## ► Stellar Masses

- determined from observations of binary systems
- FAME: 2-3 orders of magnitude improvement

## ► Stellar Luminosities

- coverage of all spectral types(!)
- refine the mass-luminosity-metallicity-age relation
- definitive absolute magnitude calibrations of early spectral types (O-A)
- allows determination of distances and ages of Galactic & extragalactic globular clusters
- constraints on stellar evolution theories & models

## ► Evolution of Interacting Binary Systems

- novae & nova-like variables
- Be star x-ray binary systems
- Wolf-Rayet stars
- LMXRBs
- problem: current paucity of definitive mass and orbit determinations

# FAME Science Highlights

---

## ► Exotic Objects

- black hole candidates within reach of FAME:

	$m_v$	d (kpc)	$M/M_{\text{sun}}$	$\sigma_d$ (%)
V616 Mon	11.3-20	1.0	>3-9	5
Nova Mus 1991	13.4-20	1.4	?	20
Cyg X-1	9	2.5	9	7
V404 Cyg	11.5-18	1-3	8-15?	5-15

## ► Global Reference Frame

- FK5: ~10 mas at epoch ~1940
- optical/radio frame disparity ~10 mas
- with proper motion errors, ~10 mas at time of FAME
- FAME: ~50  $\mu\text{as}$ , tied to radio frame

# FAME Science Highlights

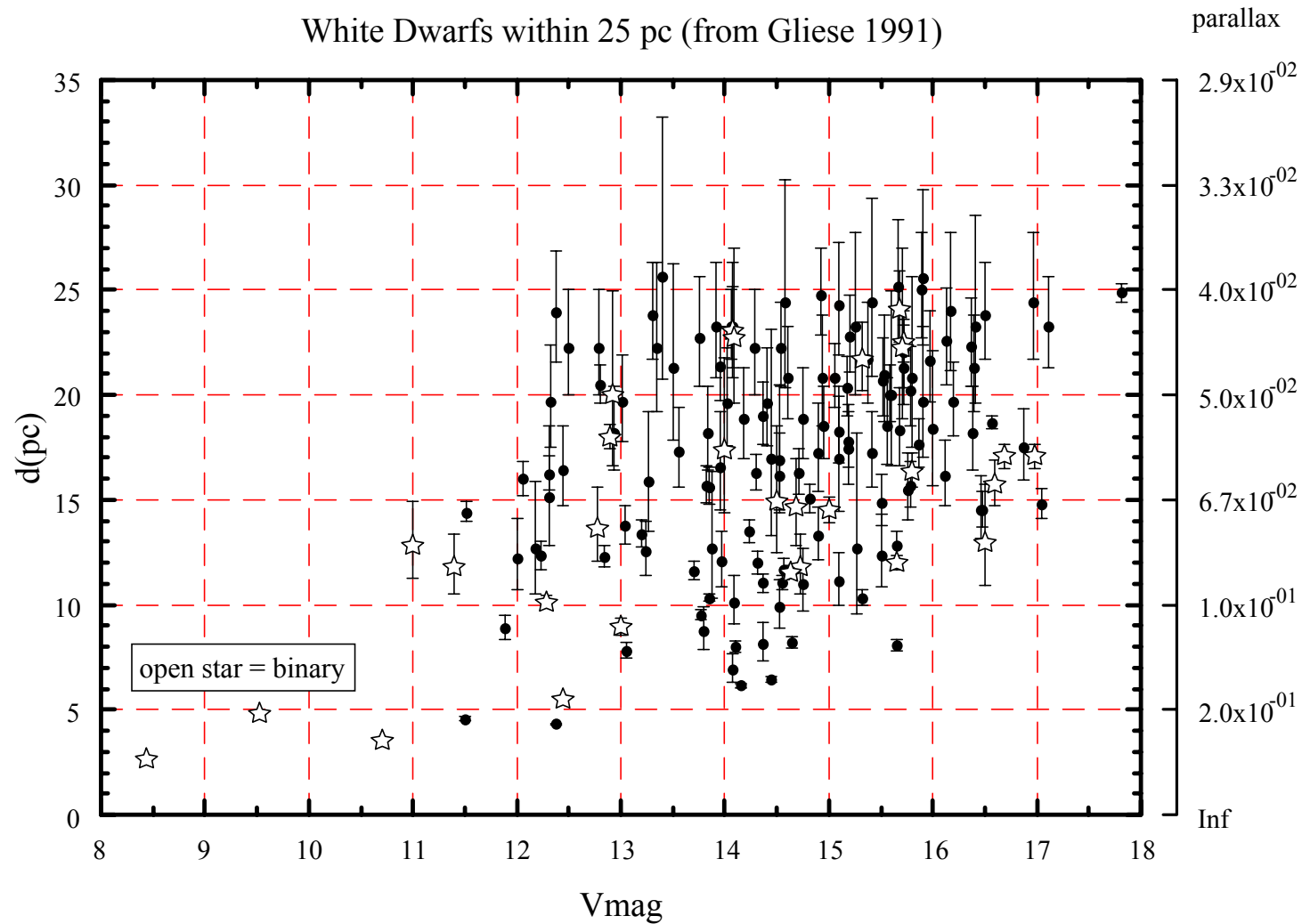
---

## ► White Dwarfs

- distances currently very uncertain
- 162 known within 25 pc
- M-R relation poorly calibrated, due mostly to uncertain distances
- mass distribution has implications for
  - progenitor population(s)
  - Galactic evolution
- FAME would nail the WD distance problem.

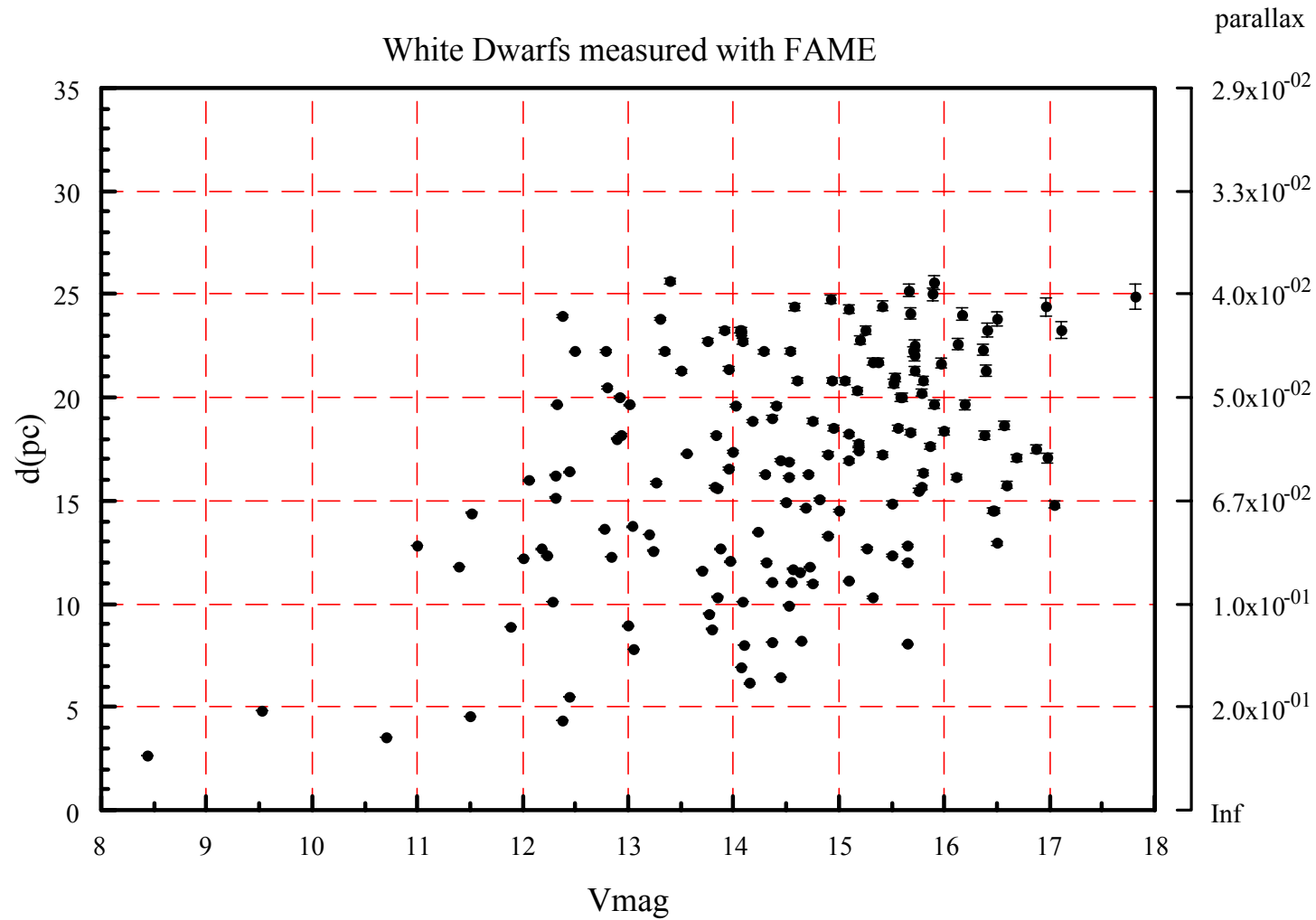
# FAME Science Highlights

## ► White dwarf distances:



# FAME Science Highlights

## ► What FAME could do:



# FAME Science Highlights

---

## ► Substellar object detection

- Orbital periods up to a bit longer than the mission duration
- Definitive determination of the frequency of solar-type stars orbited by brown dwarf companions in the mass range 10 to 80 M<sub>Jup</sub>
- Exploration of the transition region between giant planets and brown dwarfs
  - ~10-30 M<sub>Jup</sub>
- A 5-year mission could detect Jupiters in ~0.2-10 AU orbits around stars less than ~10 pc away



# Constraints on astrometric accuracies due to the observation scanning pattern

# What Determines Mission Accuracies?

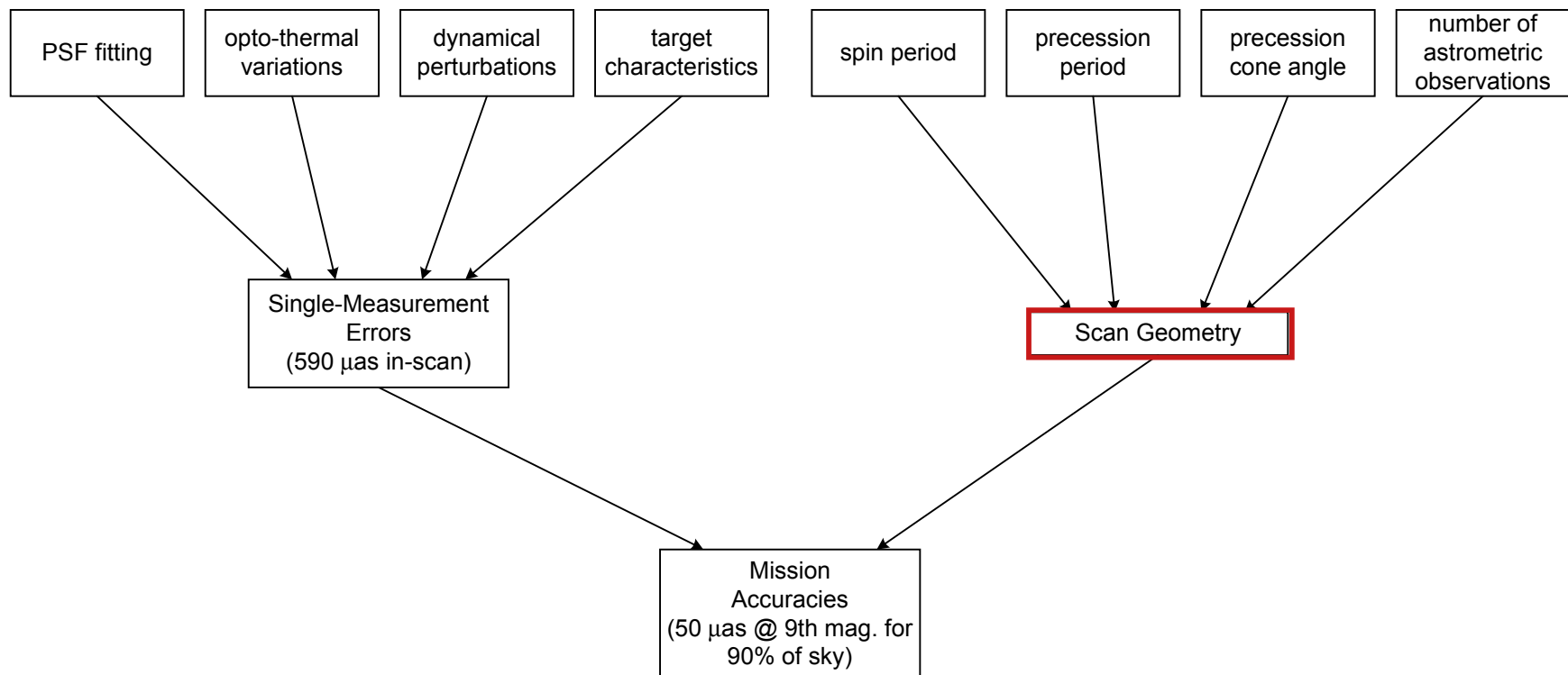
---

- ▶ Broadly speaking, we have "global" and "local" considerations
- ▶ Local
  - instrumental parameters and characteristics
  - detailed dynamical and orbital motions
  - this category contains all the physics
  - affects single-measurement accuracies
  - subject of another talk
- ▶ Global
  - driven entirely by the scanning geometry
  - two important distributions
    - distribution of observation density (a function of position on the sky)
    - distribution of scan angles (also a function of sky position)
      - ▶ scan angle: at a given point on the sky, the angle that the telescope FOV motion makes wrt an ecliptic meridian through that point
  - sets **upper bounds** on the mission-averaged accuracies that the instrument can achieve, given
    - the instrument geometry
    - a statistical description of the single-measurement errors

# What Determines Mission Accuracies?

---

- ▶ nitty-gritties contribute to single-measurement errors ("local")
- ▶ observation density and scan angle distributions determined by scan geometry ("global")

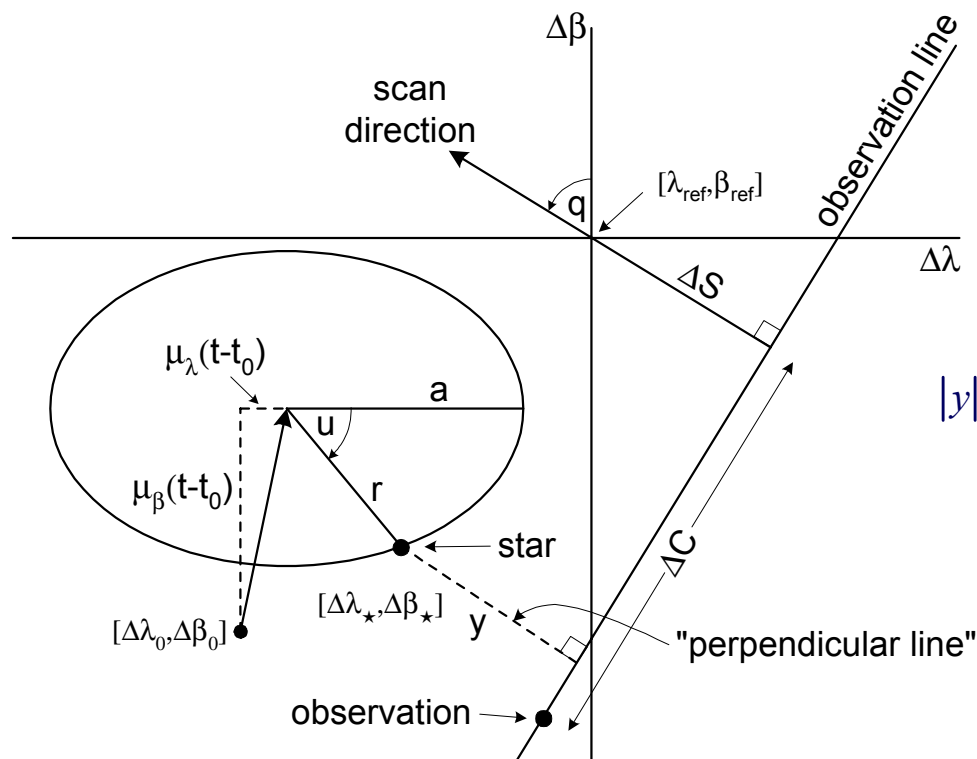


# Global Geometry Trade Study

---

- ▶ Determine optimum scanning parameters
  - Precession cone angle
  - Precession period
  - Spin period
- ▶ Combined analytical and numerical approach
- ▶ Numerical program
  - accurately simulates scanning pattern on the sky
  - assumes a value for the  $1\sigma$  scan-direction single-measurement error
  - accumulates "observations" on an equal-area grid
  - performs statistical analyses on grid cell data
  - includes relevant instrument features
    - 2 viewports
    - basic angle
    - individual CCDs arranged in columns on the focal plane

# Observation Geometry



$$|y| \simeq \left| \Delta S - a [\sin(\lambda_{ref} - \lambda_{\odot}) \sin q + \sin \beta_{ref} \cos(\lambda_{ref} - \lambda_{\odot}) \cos q] + [\Delta \beta_0 + (t - t_0) \mu_{\beta}] \cos q - [\Delta \lambda_0 + (t - t_0) \mu_{\lambda}] \sin q \right|$$

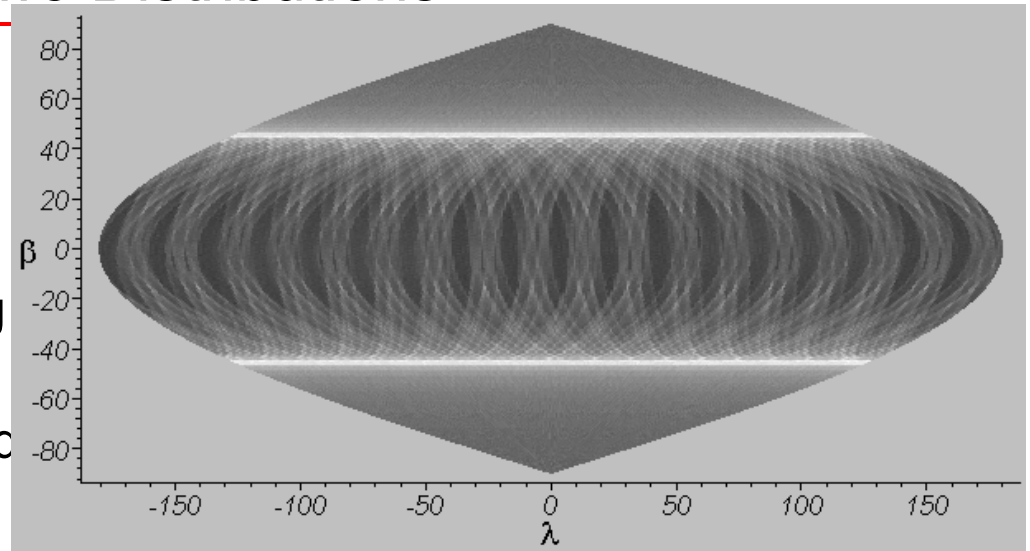
The instrument makes an observation of a star, deriving  $\Delta S$  and  $\Delta C$  (scan and cross-scan positions) with respect to local ecliptic coordinates  $[\Delta \lambda, \Delta \beta]$  located on the sky at  $[\lambda_{ref}, \beta_{ref}]$ . Scan direction is indicated, making an angle  $q$  wrt the local ecliptic meridian ( $\Delta \beta$  axis). The observation point is not coincident with the star due to single-measurement errors. Measurement errors are in general orders of magnitude worse cross-scan than in-scan, causing the measurement error ellipse to be *extremely* elongated. We therefore approximate it as the limiting case: an "observation line". (Note that  $\Delta C$  is not drawn to scale in the figure.) Given a number of observations, the distance  $y$  of the observation lines from the true location of the star then becomes the most natural quantity to minimize in a least squares sense.

Due to Earth's orbital motion, the star moves on an ellipse on the sky, with semimajor axis  $a$  and eccentricity  $\cos \beta$ . Due to proper motion  $[\mu_{\lambda}, \mu_{\beta}]$ , the center of the ellipse moves during the mission. The least squares algorithm minimizes the length of the perpendicular line segment  $y$  by solving for the astrometric parameters: (1) the position  $[\Delta \lambda_0, \Delta \beta_0]$  of the ellipse center at epoch  $t_0$ , (2) the proper motion components  $[\mu_{\lambda}, \mu_{\beta}]$ , and (3) the semimajor axis  $a$  of the parallactic ellipse. The resulting covariance matrix then yields the formal errors and cross-correlations of the parameters.

# General Characteristics of the Two Distributions

## ► Observation density distribution

- highest density at top & bottom of precession cone holes (which smear in longitude), corresponding to two zones in latitude  $|\beta| = 90 - \psi$
- lowest densities are in ecliptic band between the high-density zones
- ecliptic band exhibits density "ribbing" corresponding to the times when the spacecraft spin axis lies in ecliptic plane
  - best accuracies in the mid-latitude high-density zones
  - worst accuracies in the ecliptic band
  - ecliptic band is not uniformly bad



## ► Scan angle distribution

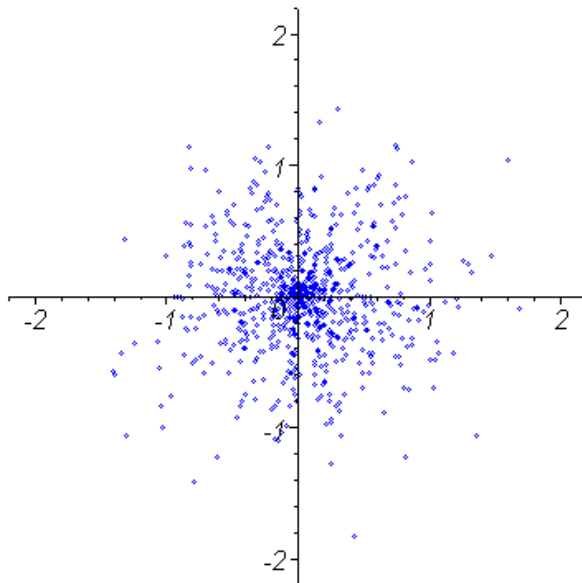
- homogeneous in polar cap regions (latitudes above high-density zones)
- cone-shaped on ecliptic, with cone opening angle  $90 - \psi$ 
  - better position accuracies in polar cap regions
  - longitude position accuracy substantially degraded near ecliptic
  - latitude position accuracy slightly degraded near ecliptic
  - better parallax accuracy in polar cap regions

# Scan Angle Distribution Snapshots

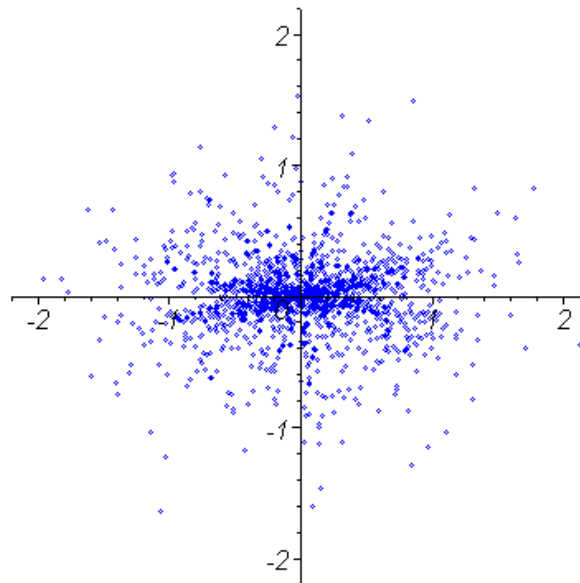
---

- scatterplots in ecliptic coordinates
  - scale is milliarcseconds
  - along-scan single-observation errors: Gaussian distribution with  $1\sigma = 0.6$  mas

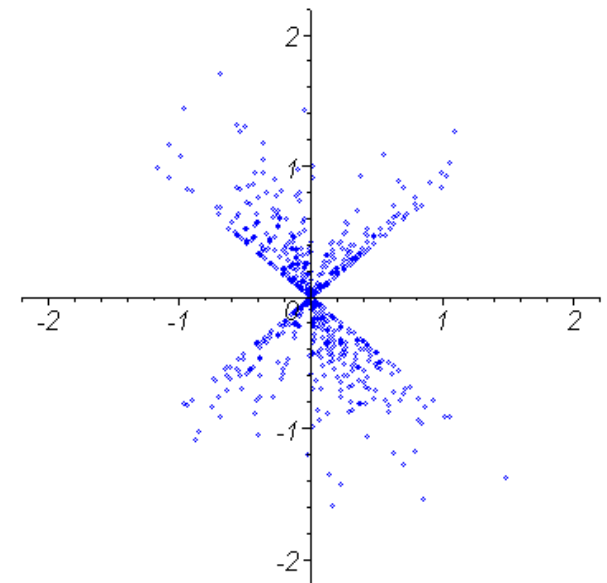
high latitude



mid-latitude

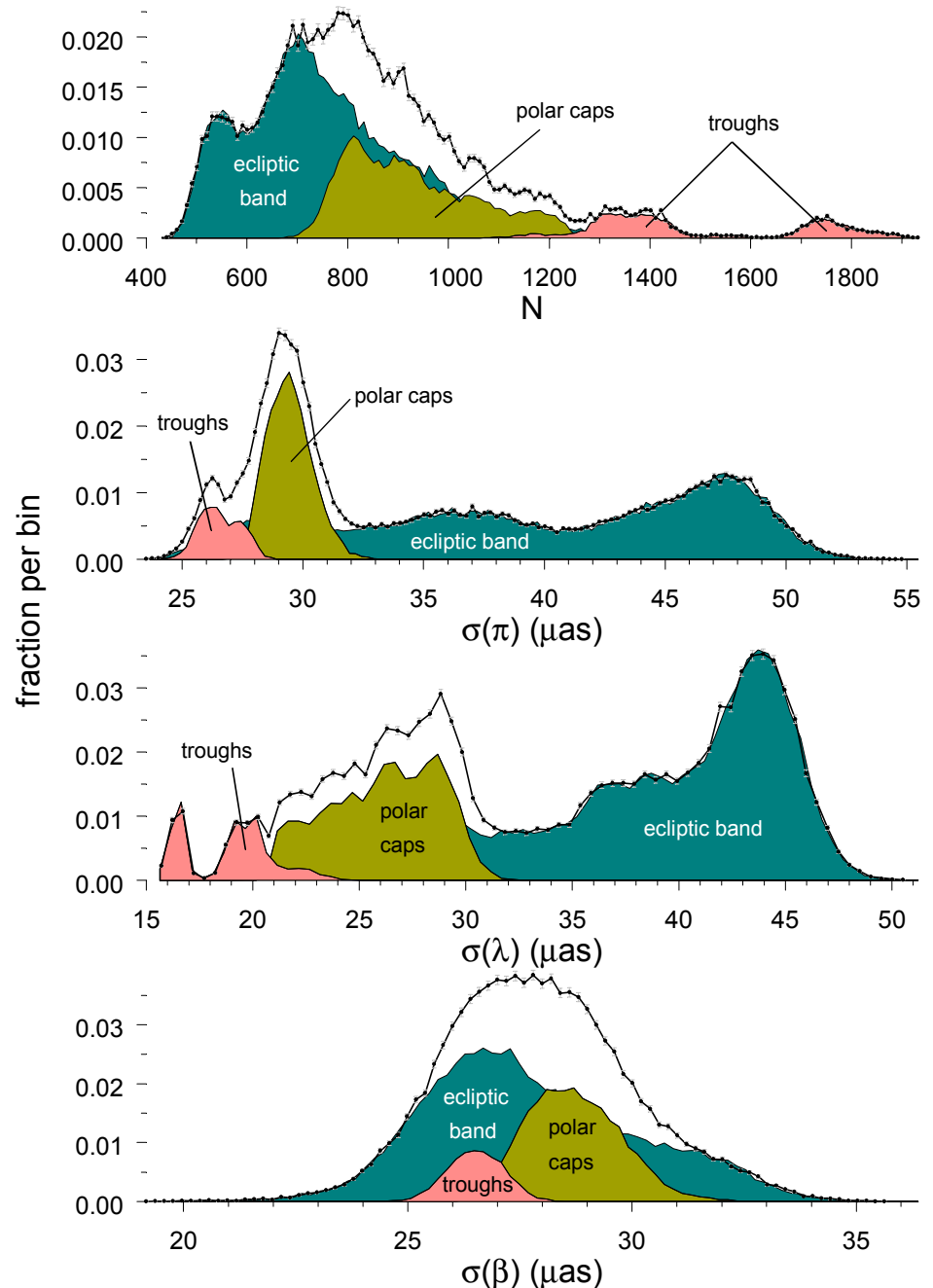


low latitude



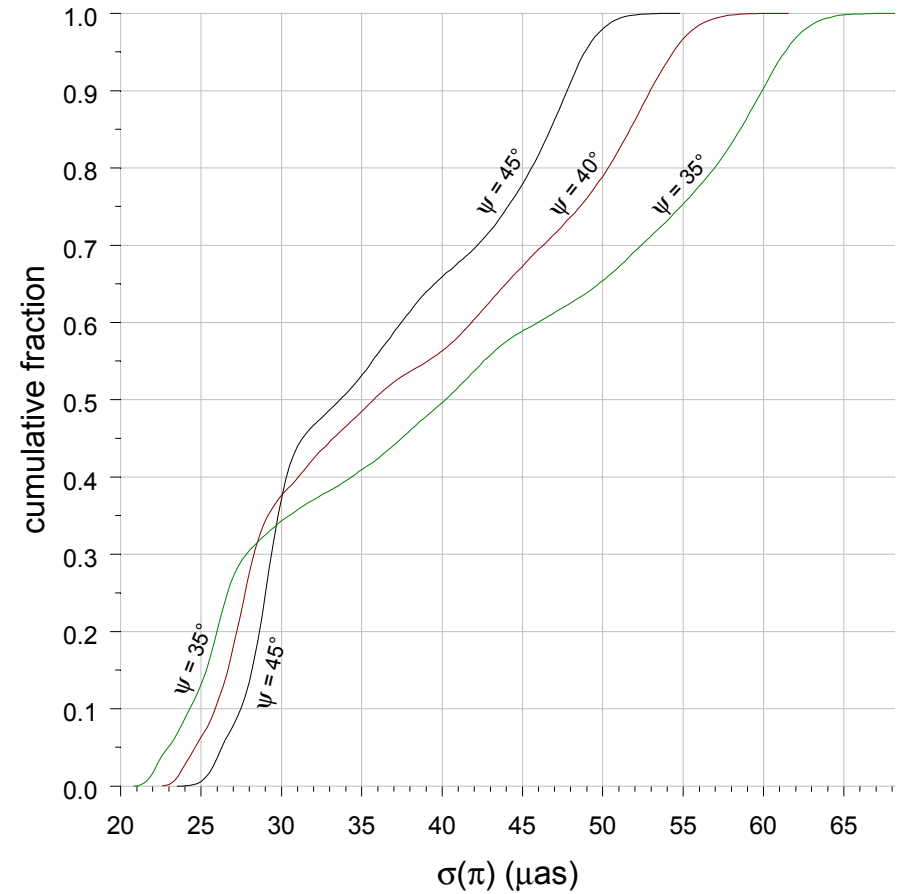
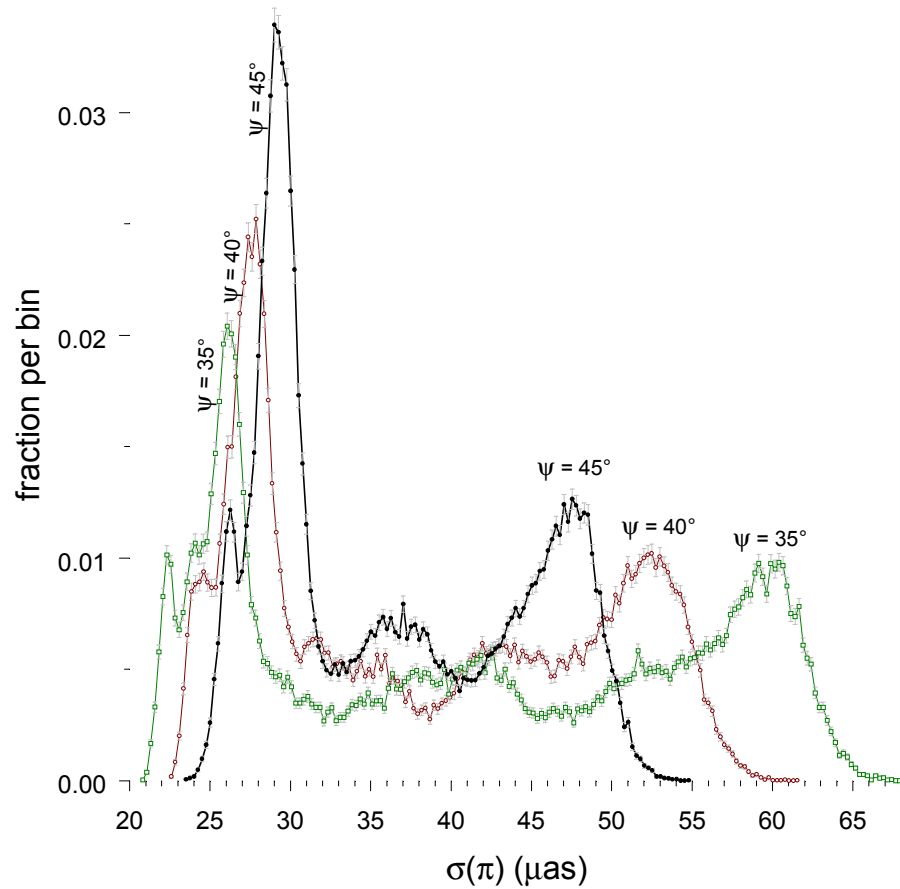
# Components of Histograms and their Behavior

- sky naturally divided by scanning geometry into distinct regions:
  - high-density troughs at  $|\beta| = 90 - \psi$
  - ecliptic band  $|\beta| < 90 - \psi$
  - polar caps  $|\beta| > 90 - \psi$
- as Sun angle decreases:
  - polar caps shrink
  - ecliptic band grows
  - longitude
    - high-accuracy population shrinks, moves left
    - low-accuracy population grows, moves right
  - latitude
    - distribution broadens and peak moves left
  - parallax
    - main feature shrinks, moves left
    - poor-accuracy fraction grows

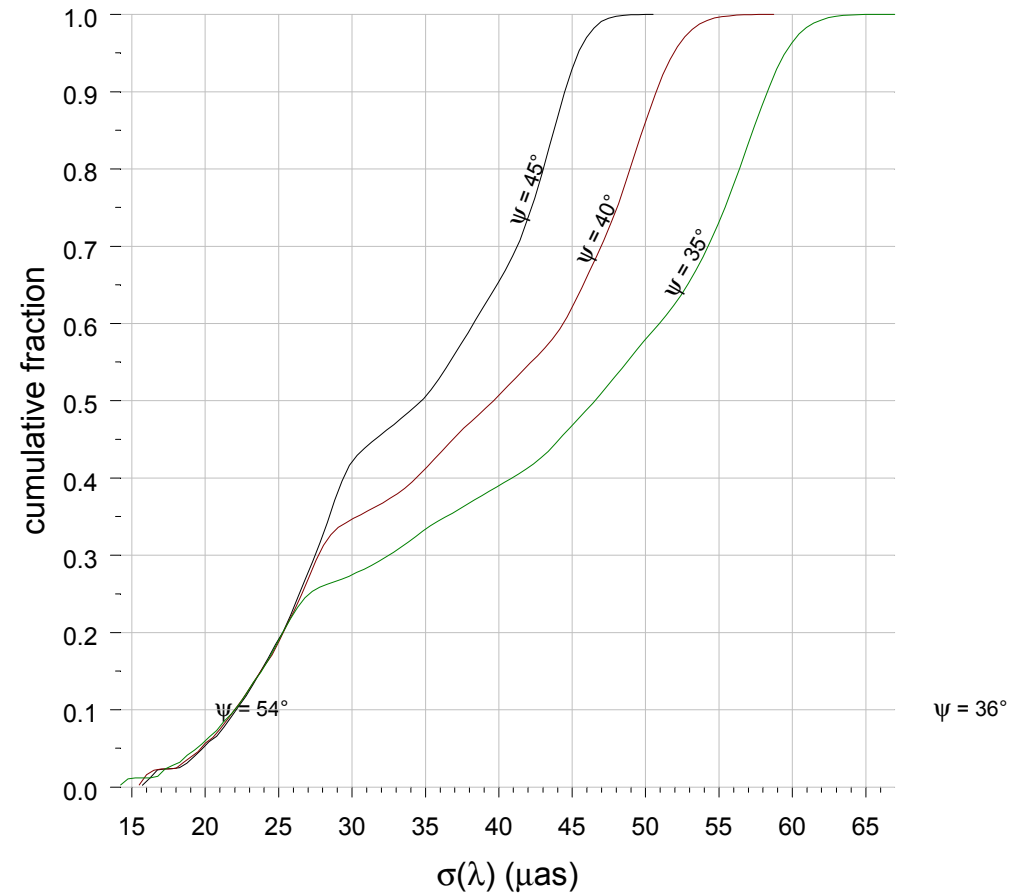
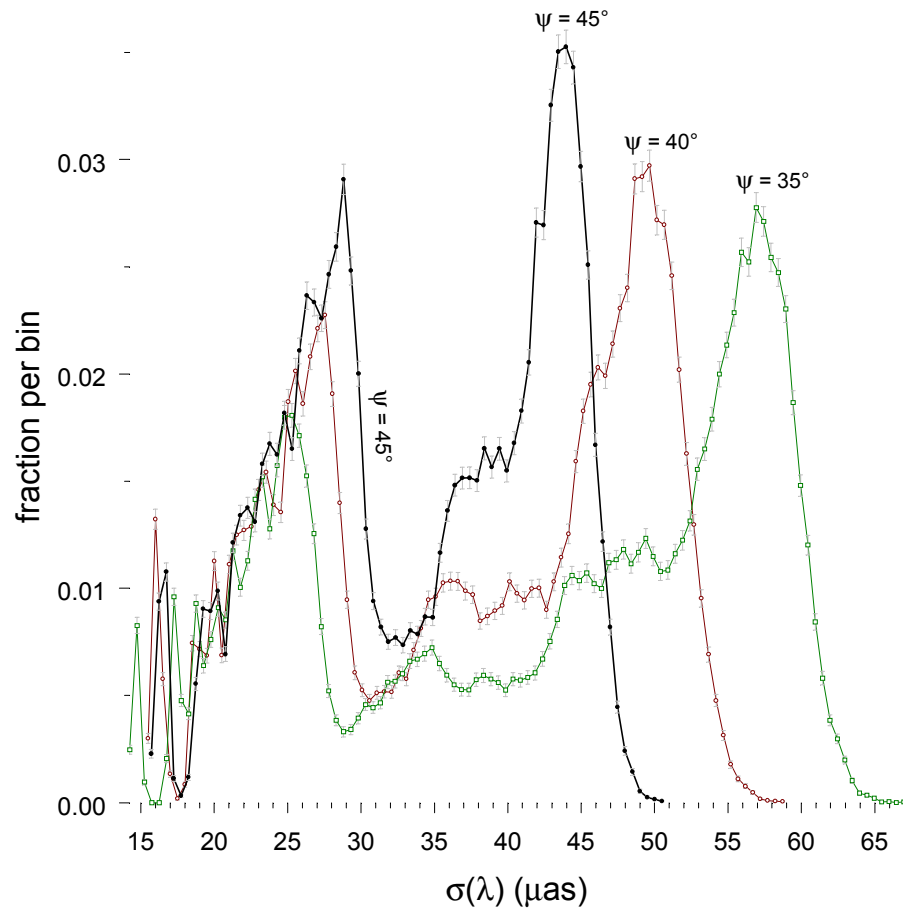




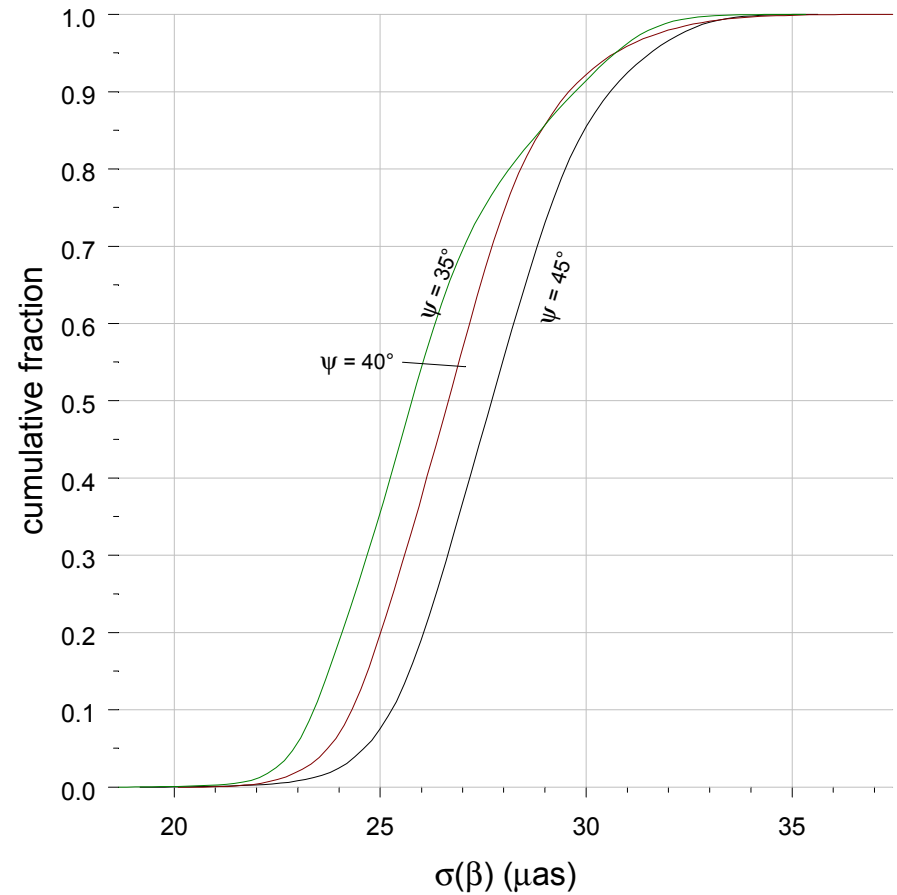
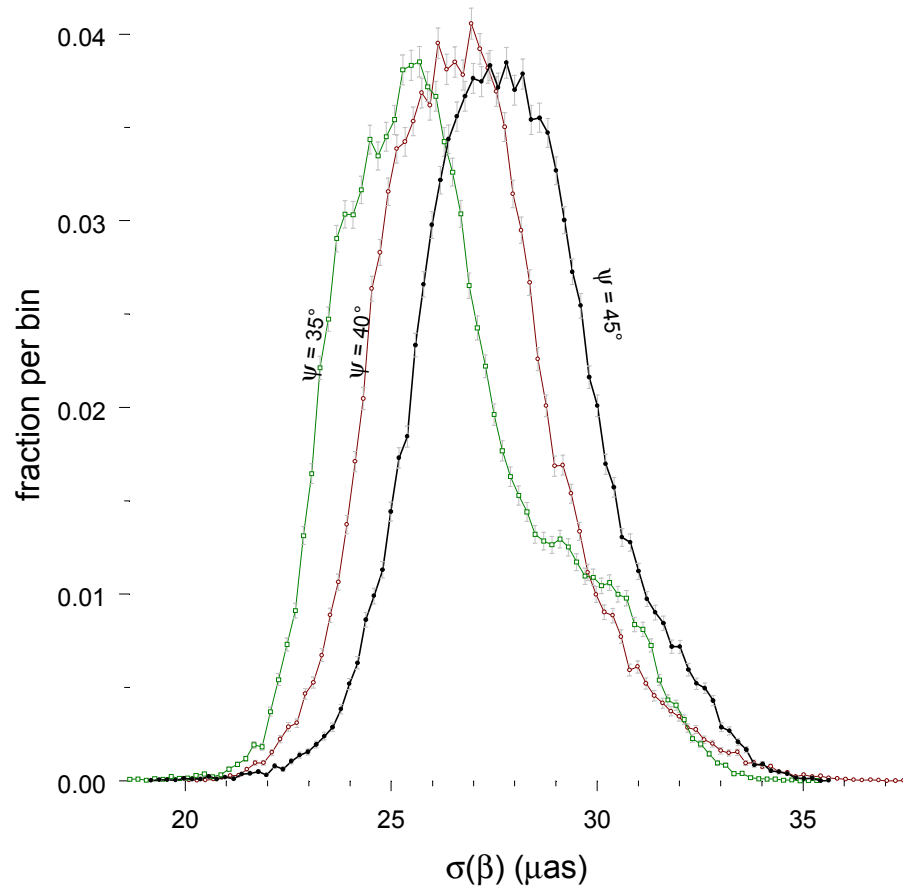
# Histograms: Errors in Parallax



# Histograms: Errors in Ecliptic Longitude



# Histograms: Errors in Ecliptic Latitude



## Sky Percentages that Meet Mission Goals

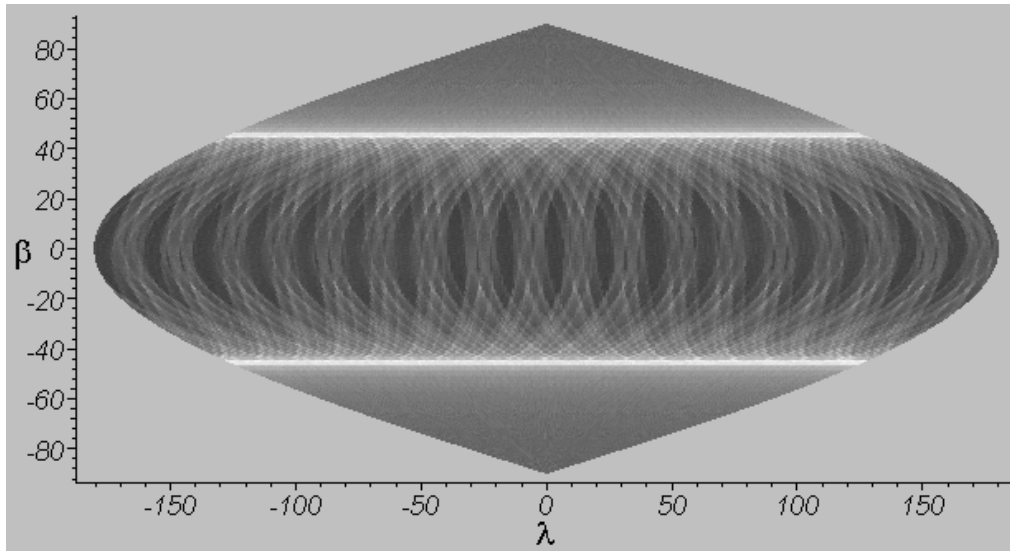
---

- The table below shows percentages of the sky for which a 2.5 year FAME mission can meet or do better than the goals of 50  $\mu\text{as}$  (position, parallax) and 50  $\mu\text{as/yr}$  (proper motion), for three nominal Sun angles and assuming a 590  $\mu\text{as}$  single-measurement standard error.

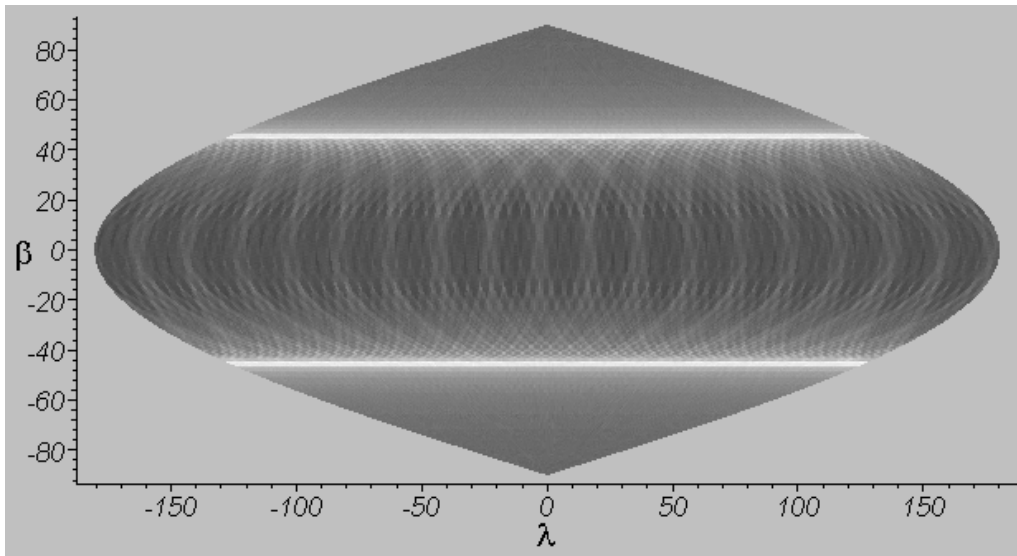
	45 degrees	40 degrees	35 degrees
parallax	98	79	65
position — longitude	100	86	58
position — latitude	100	100	100
pm — longitude	54	43	33
pm — latitude	100	100	100

## 5-Year Observation Density Distribution

---

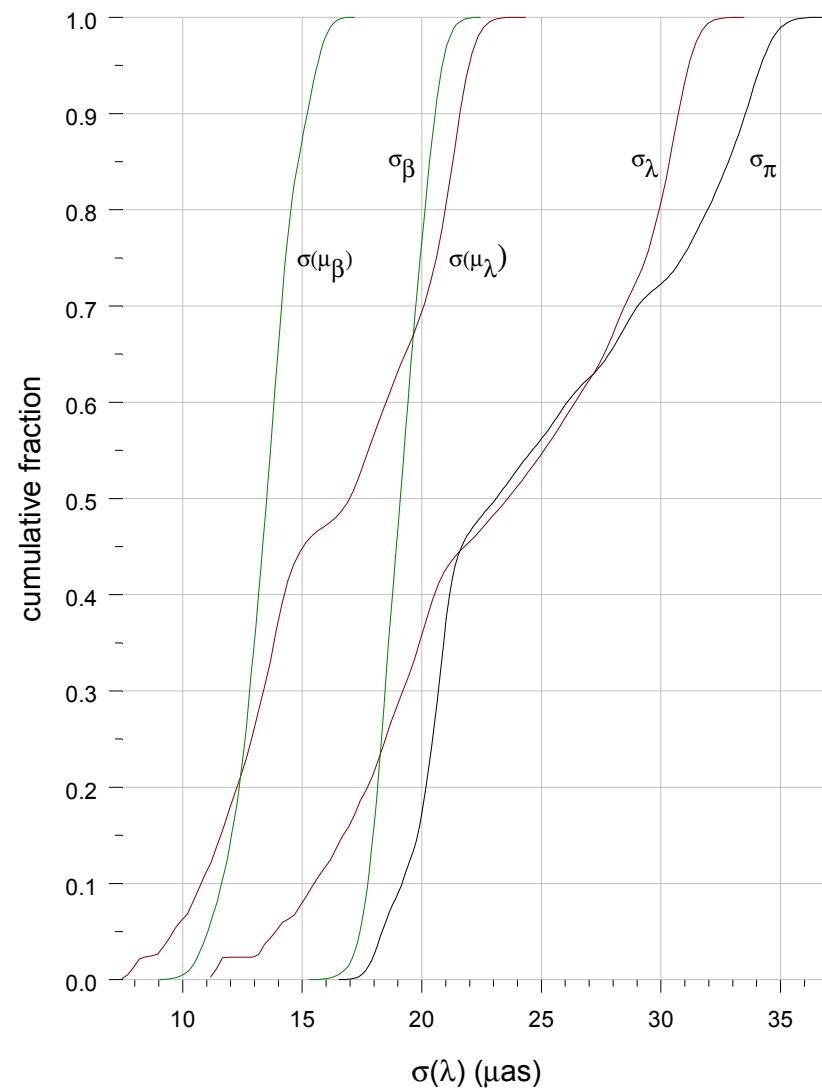
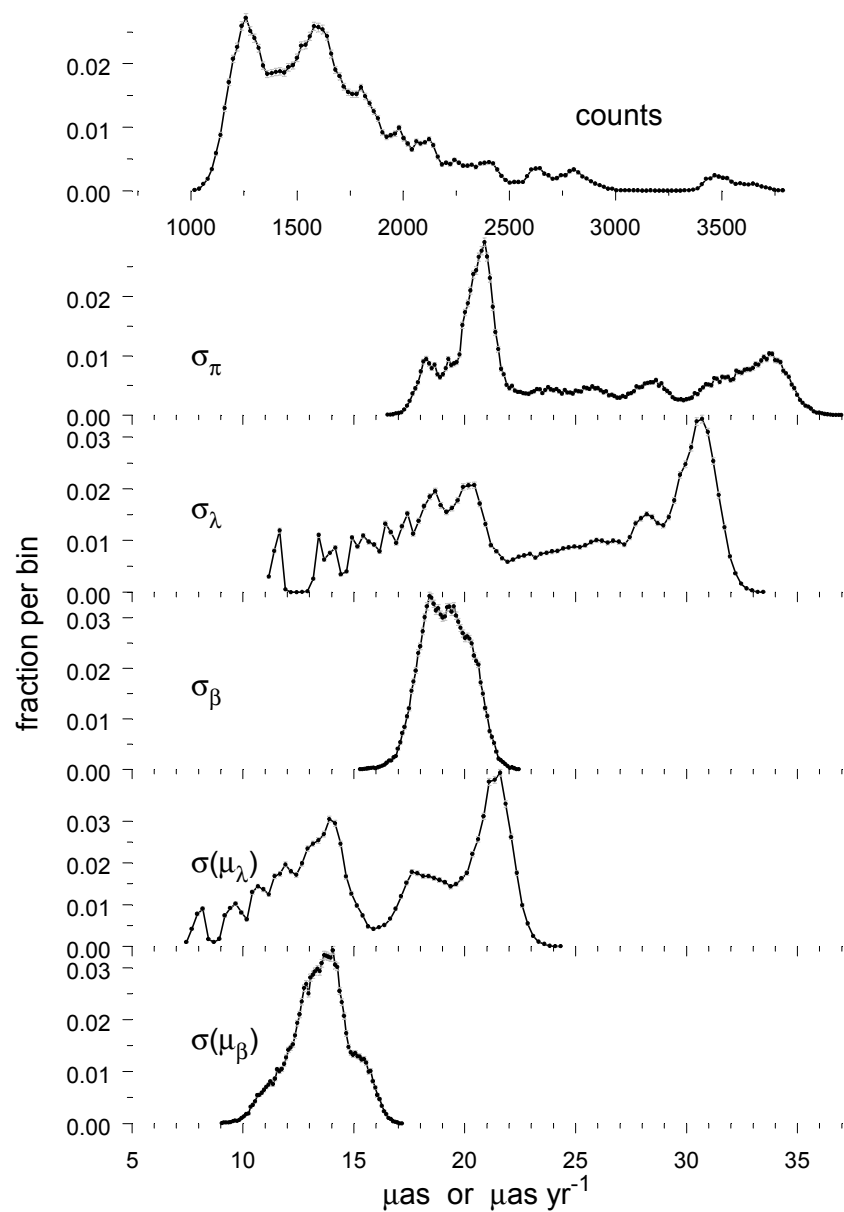


2.5 years



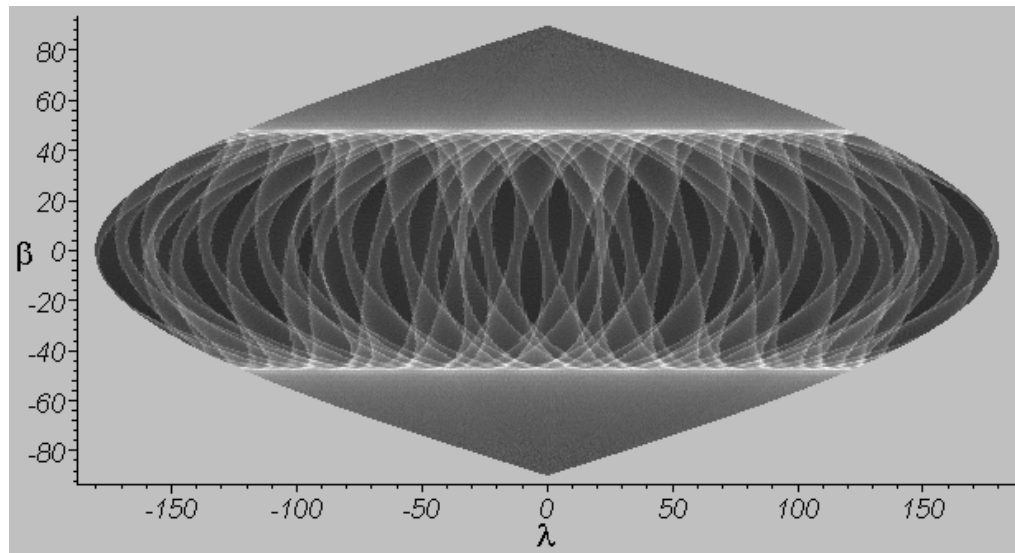
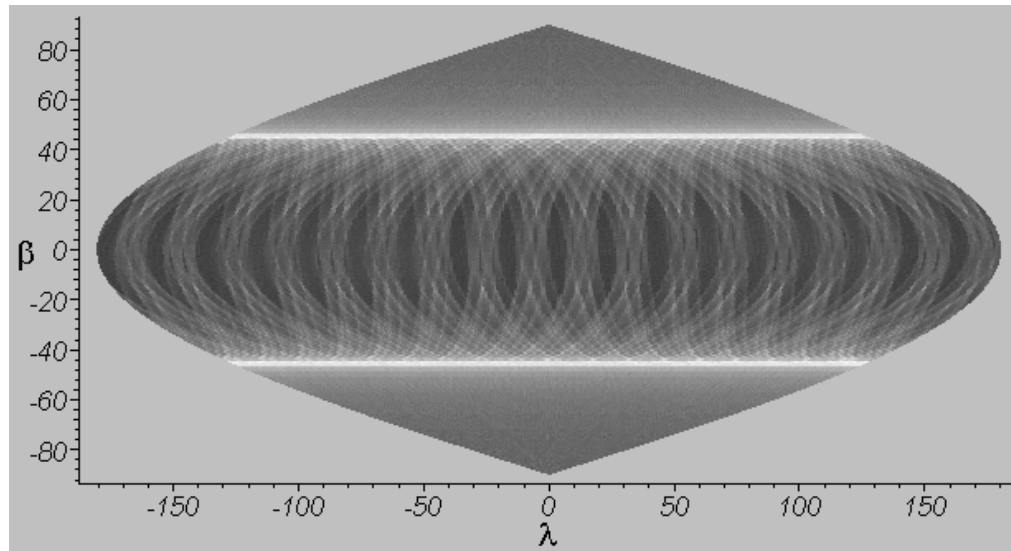
5 years

# 5-Year Mission Histograms



# FAME vs. Hipparcos

---



# Consequences of solar irradiance fluctuations



# Introduction

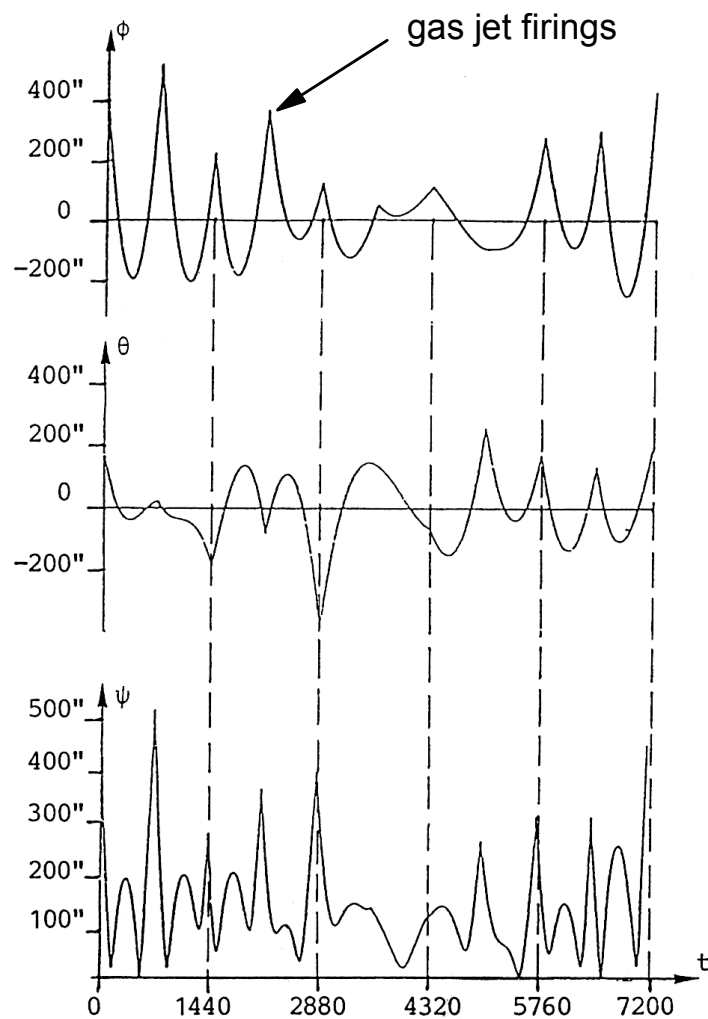
---

- ▶ FAME satellite's precession will be driven by solar radiation pressure on the spacecraft's sun shield
- ▶ Advantage: continuity of data, resulting in increased mission accuracy
  - SAO group covariance studies (FTM99-05)
    - gain a factor of 4 in rotation coherence in going from 6 thruster firings per rotation to one firing per rotation
    - asymptotic limit: one order of magnitude accuracy gain
- ▶ Potential problem: irradiance fluctuations
  - Stochastic, therefore potentially unmodelable
- ▶ How can we reduce the impact from stochastic perturbations?
  - spin faster
  - reduce shield size
  - increase s/c mass or significantly alter the s/c mass distribution
- ▶ Key Question: What is the character and magnitude of the effects of solar irradiance fluctuations on the spacecraft spin dynamics, and hence the effects on measurement accuracy?

# Hipparcos Attitude Corrections

---

- This is why we don't want thruster firings
- Plot scale is arc seconds



# Introduction (continued)

---

## ► What the problem entails:

- Understanding of rigid body dynamics
- Development of a useful torque model
  - Pressure field model(s)
    - Solar wind (not a problem in geosynchronous orbit)
    - Solar radiation pressure — three approaches:
      - constant magnitude (bad approx.)
      - model the fluctuations (very difficult solar physics problem)
      - incorporate observational data (best way to go)
    - Earth radiation pressure (not considered in this study)
  - Spacecraft solar shield model
    - Smooth "skirt", swept back by an adjustable angle to control the precession rate (Reasenberg 1997, FTM97-05)
    - Fully analytic exact solution for the torque on such a shield (Murison 1998, DDA Charlottesville, <http://aa.usno.navy.mil/murison/talks/> )
- Numerical program: exploration tool
  - see <http://aa.usno.navy.mil/SymTop/>
- Determine the effects on spacecraft attitude and measurement accuracy

# Spacecraft Spin Dynamics

---

- ▶ Start with rigid body equations of motion
- ▶ Full dynamical problem: guiding center motion around the sun direction
  - Reasenberg (1999) and V. Slabinsky (1976) (now at USNO) both independently discovered this solution
  - Simplifications for this particular study:
    - Fix the Sun in place and ignore Earth's orbital motion
    - Ignore s/c orbit around Earth
      - ▶ Earth and lunar perturbations
      - ▶ eclipses
      - ▶ gravity gradient torques
      - ▶ etc., etc., etc.
  - ➔ ignore all smooth (and therefore modelable, and therefore removable from the data) perturbations
- ▶ Simplified problem: spinning, symmetric top, with attached conical shield, embedded in a radiation pressure field
  - Ignore solar wind (magnetosphere protection)
  - Integrate pressure field over cylinder "top" and solar shield to get torques

# The Equations of Motion

---

$$\begin{aligned}
 \frac{d\varphi}{dt} &= \Omega_\varphi \\
 \frac{d\psi}{dt} &= \Omega_\psi \\
 \frac{d\varphi}{dt} &= \Omega_\varphi \\
 \sin \psi \frac{d}{dt} \Omega_\varphi &= [(1-\beta) \Omega_\theta - (1+\beta) \cos \psi \Omega_\varphi] \Omega_\psi + K_1(a, b, h, a, A_C, A_T, \varphi, \psi) \\
 \frac{d}{dt} \Omega_\psi &= [\beta \cos \psi \Omega_\varphi^2 - (1-\beta) \Omega_\theta \Omega_\varphi] \sin \psi + K_2(a, b, h, a, A_C, A_T, \varphi, \psi) \\
 \sin \psi \frac{d}{dt} \Omega_\theta &= [(1+\beta \cos^2 \psi) \Omega_\varphi - (1-\beta) \cos \psi \Omega_\theta] \Omega_\psi + K_3(a, b, h, a, A_C, A_T, \varphi, \psi)
 \end{aligned}$$

$$\begin{aligned}
 K_1(a, b, h, a, A_C, A_T, \varphi, \psi) &\equiv G(a, b, h, a, A_C, A_T) \cdot g_1(\varphi, \psi) \\
 K_2(a, b, h, a, A_C, A_T, \varphi, \psi) &\equiv G(a, b, h, a, A_C, A_T) \cdot g_2(\varphi, \psi) \\
 K_3(a, b, h, a, A_C, A_T, \varphi, \psi) &\equiv G(a, b, h, a, A_C, A_T) \cdot g_3(\varphi, \psi)
 \end{aligned}$$

$$\begin{aligned}
 g_0(\varphi, \psi) &= -\pi_X \sin \varphi \sin \psi + \pi_Y \sin \psi \cos \varphi - \pi_Z \cos \psi \\
 g_1(\varphi, \psi) &= g_0(\varphi, \psi) \cdot (\pi_X \cos \varphi + \pi_Y \sin \varphi) \\
 g_2(\varphi, \psi) &= g_0(\varphi, \psi) \cdot (\pi_X \cos \psi \sin \varphi - \pi_Y \cos \psi \cos \varphi - \pi_Z \sin \psi) \\
 g_3(\varphi, \psi) &= -g_1(\varphi, \psi) \cos \psi
 \end{aligned}$$

$$\begin{aligned}
 G(a, b, h, a, A_C, A_T) &= G_C(a, b, h, a, A_C) + G_T(a, h, A_T) \\
 G_C(a, b, h, a, A_C) &= \frac{\pi P}{I_{xy}} (b-a) \left[ (1-A_C + 2A_C \cos^2 a) (h \sin a + a \cos a) \frac{a+b}{\sin a} \right. \\
 &\quad \left. - \frac{1}{3} (3+A_C) \cos a \frac{a^2 + ab + b^2}{\sin a} \right] \\
 G_T(a, h, A_T) &= \frac{\pi P}{I_{xy}} (1-A_T) a^2 h
 \end{aligned}$$

# Basic Dynamical Behavior

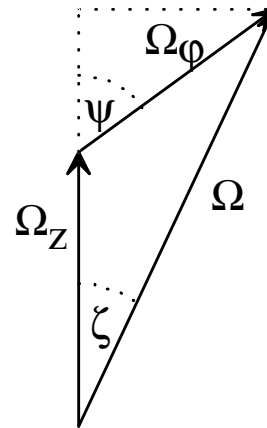
---

## ► Constant pressure field

- Smooth precession
- Constant sun angle  $\psi$
- Thump it, and it rings (nutation)
- Angular velocity along spin axis is conserved
- Angular velocity vector in the rotating spacecraft frame executes circular motion around the symmetry axis
  - Frequency
  - Radius

$$\Omega_\phi \propto \frac{P \cos \psi}{(1 - \beta)\Omega_\theta}$$

$$\frac{d}{dt} (\Omega_\theta + \Omega_\phi \cos \psi) = \frac{d}{dt} \Omega_z = 0$$



$$\Omega_z \pm \Omega_\phi \cos \psi$$

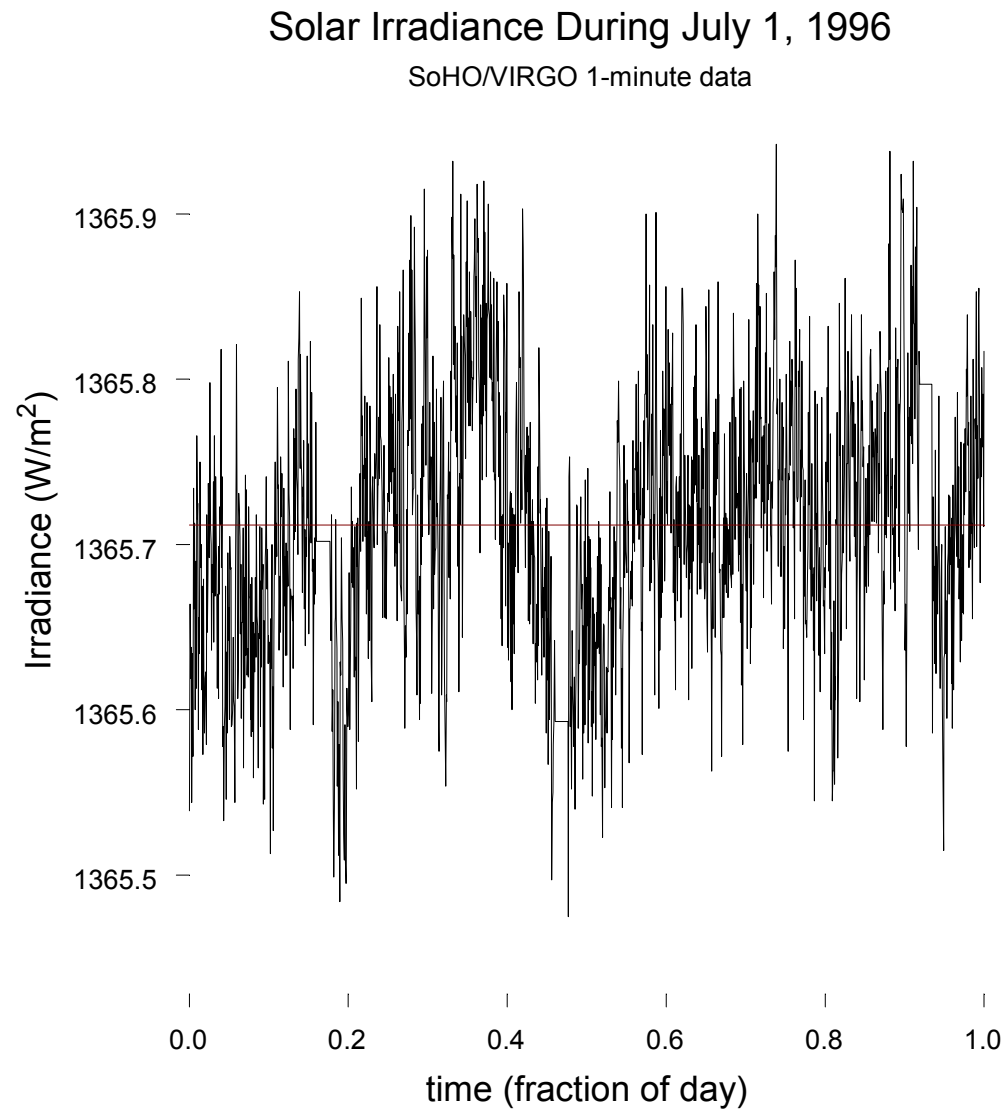
$$\tan \zeta = \frac{\Omega_\phi \sin \psi}{\Omega_z + \Omega_\phi \cos \psi}$$

## ► Time-variable pressure field

- Sun angle variations
  - variable-amplitude nutation
- Precession variations
- These variations result in "pole wandering"
- Spin ( $\Omega_z$ ) unaffected, since for solar radiation there is no net torque component along the body z axis

# Solar irradiance input

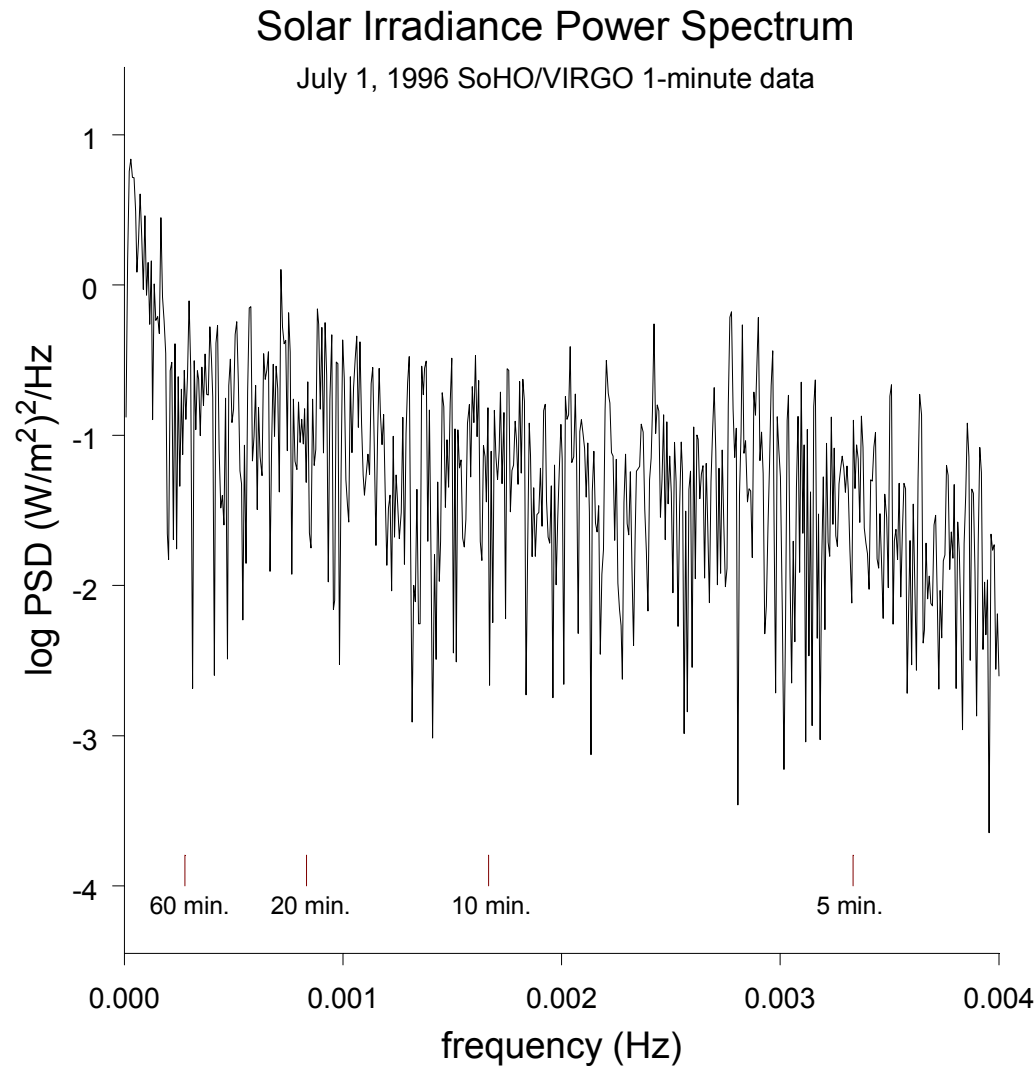
---



# Solar irradiance input

---

- Real power at all frequencies
  - Power at high frequencies is due to p-mode oscillations





# Solar Irradiance — General Properties

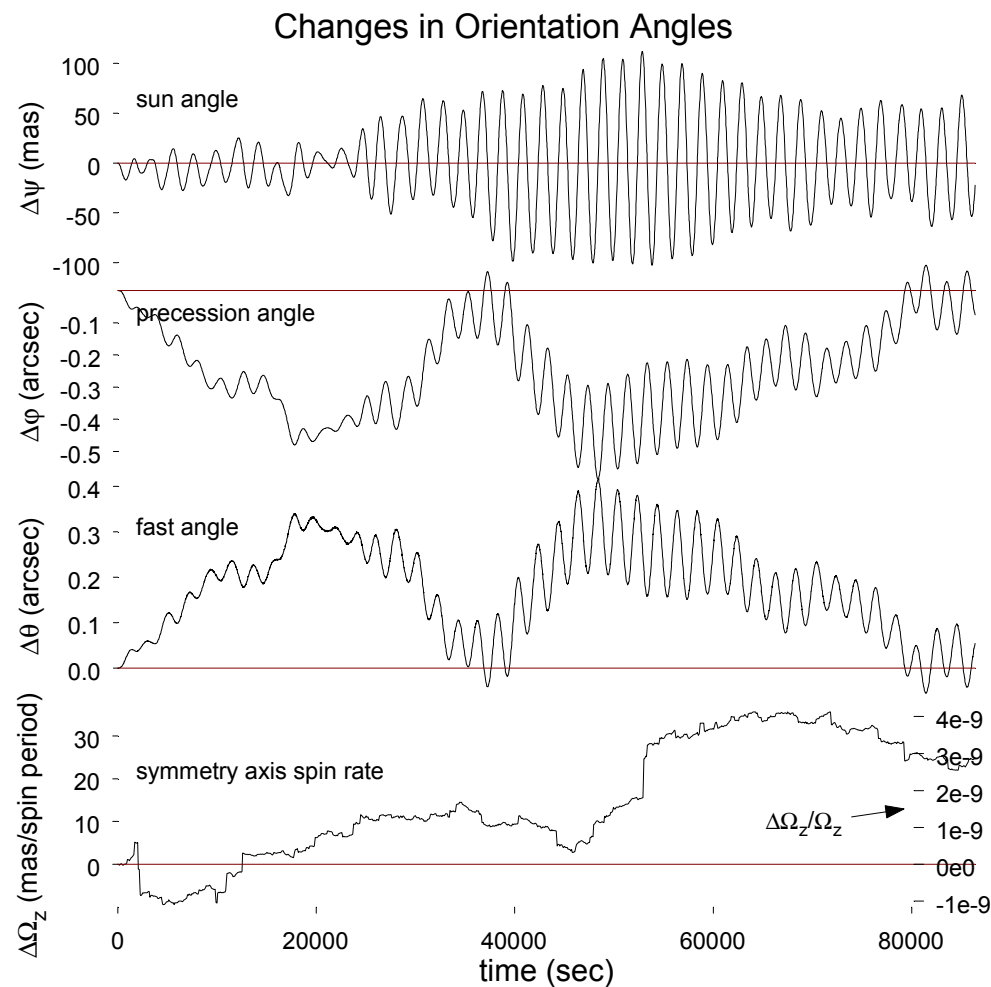
---

## ► Characteristic irradiance variations

- In general, power below 1  $\mu\text{Hz}$  is due to active regions.
- Most of the signal is at very low frequencies, around 0.4-0.5  $\mu\text{Hz}$  (~23-30 days). This corresponds to the solar rotation synodic period of ~27 days and represents the variations due to sunspot and plague regions rotating in and out of view.
- There is a significant surge of signal in the range 2000-3000  $\mu\text{Hz}$  (~5 minutes). This signal is from irradiance variations due to the 5-minute solar p-mode oscillations.
- The power in the region 10-100  $\mu\text{Hz}$  is due to supergranulation
- The power in the region 80-1000  $\mu\text{Hz}$  is due to mesogranulation.
- The power in the region 800-3000  $\mu\text{Hz}$  is due to granulation.
- See J. Pap et al., 1999, *Adv. Space Res.*, in press.
- High-order p-mode oscillations: coherence times of one to a few days (F. Varadi, 1999, private comm.)

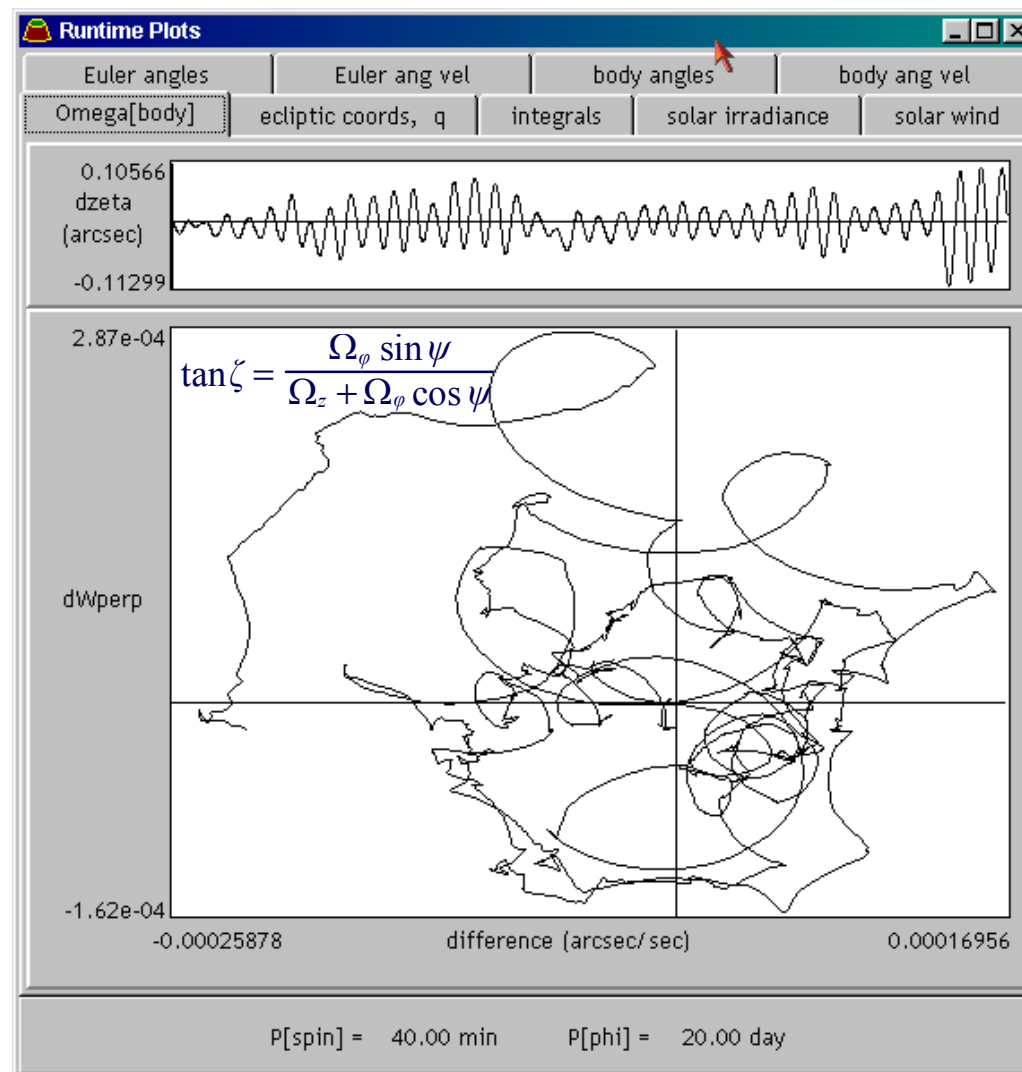
# Spacecraft Response to Solar Irradiance Fluctuations

- Orientation changes due to irradiance fluctuations
  - fast angle ( $\theta$ ) and precession angle ( $\phi$ ) changes are opposite in sign
  - spin parallel to symmetry axis ( $\Omega_z$ ) is conserved



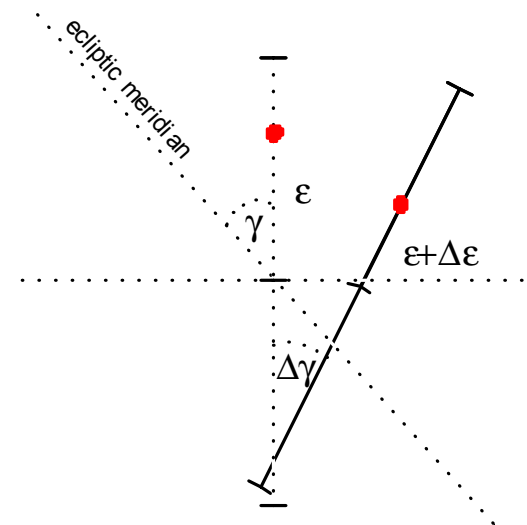
## Spacecraft Response to Solar Irradiance Fluctuations (cont.)

- Variations of perpendicular component of angular velocity vector in body frame (arcseconds/sec)



# Simulated Star Transit Observations

- ▶ Installed arbitrary number of viewports (use 2), separated by a uniform angle (81.5 degrees)
- ▶ "Detect" a star when it crosses a fiducial line segment on the focal plane
  - Project line segment onto sky
- ▶ Observables:
  - time of detection
  - cross-scan location  $\varepsilon$
- ▶ Effects of orientation fluctuation:
  - rotation of fiducial line,  $\Delta\gamma$
  - cross-scan displacement shift,  $\Delta\varepsilon$
  - these give rise to a timing error,  $\Delta t$
- ▶ Relation to integration variables (Euler angles  $\theta, \psi, \varphi$ ) is a simple problem in spherical trig.:



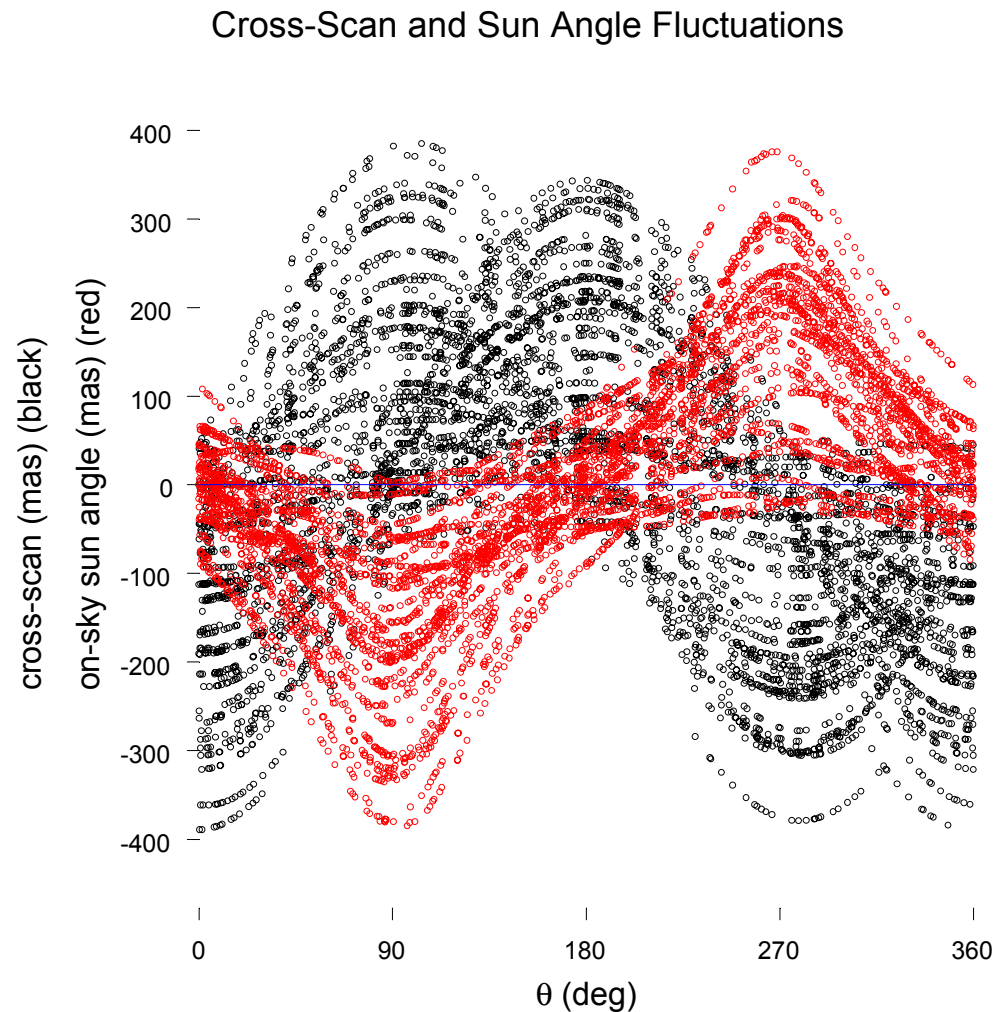
$$\begin{aligned}
 \tan \gamma &= \tan \psi \cos \theta \\
 \cos \varepsilon \cos \kappa &= \sin \psi \sin \beta \sin \theta + (\sin(\lambda - \varphi) \cos \psi \sin \theta + \cos(\lambda - \varphi) \cos \theta) \cos \beta \\
 \cos \varepsilon \sin \kappa &= \sin \psi \sin \beta \cos \theta + (\sin(\lambda - \varphi) \cos \psi \cos \theta - \cos(\lambda - \varphi) \sin \theta) \cos \beta \\
 \sin \varepsilon &= \cos \psi \sin \beta - \sin(\lambda - \varphi) \sin \psi \cos \beta
 \end{aligned}$$

where  $\kappa$  is azimuthal position of viewport

# Simulated Star Transit Observations (continued)

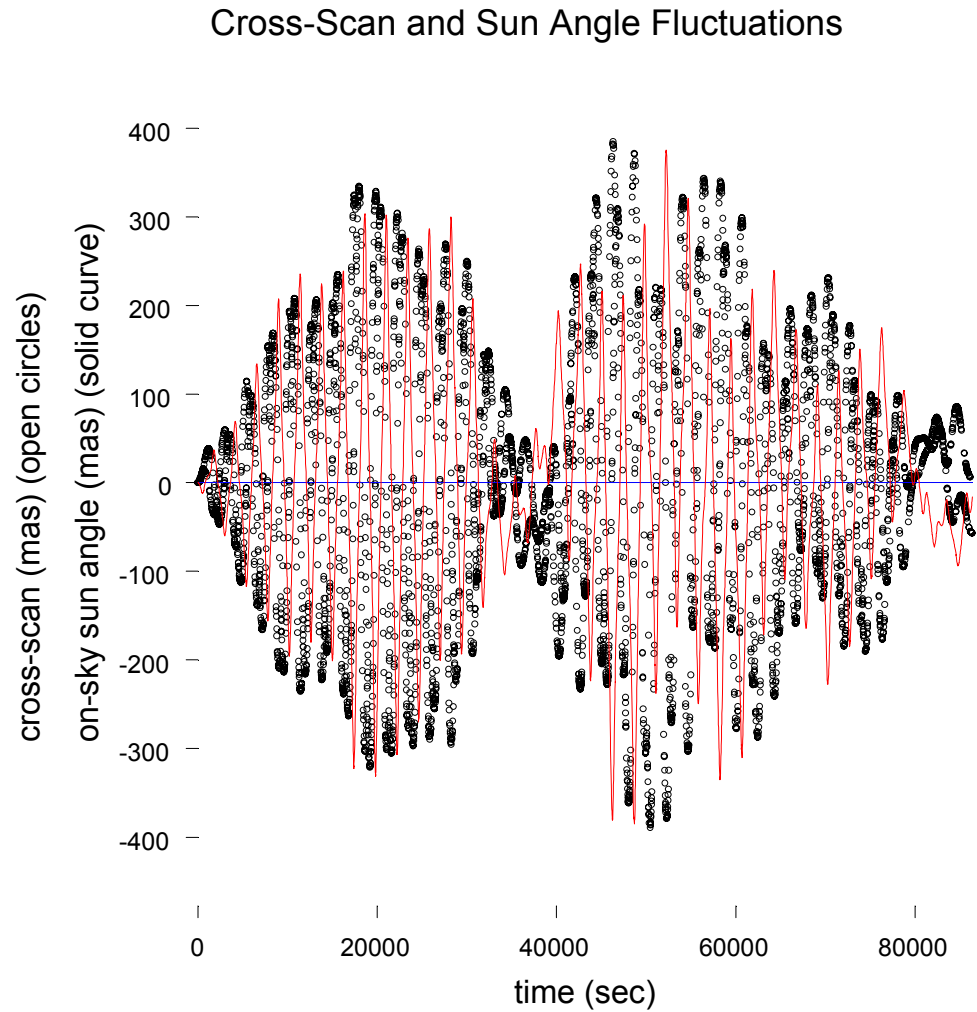
---

- Cross-scan and sun angle perturbations as a function of spin angle
  - curves behave as expected from theory (equations not shown here)



# Simulated Star Transit Observations (continued)

- Cross-scan and sun angle perturbations as a function of time

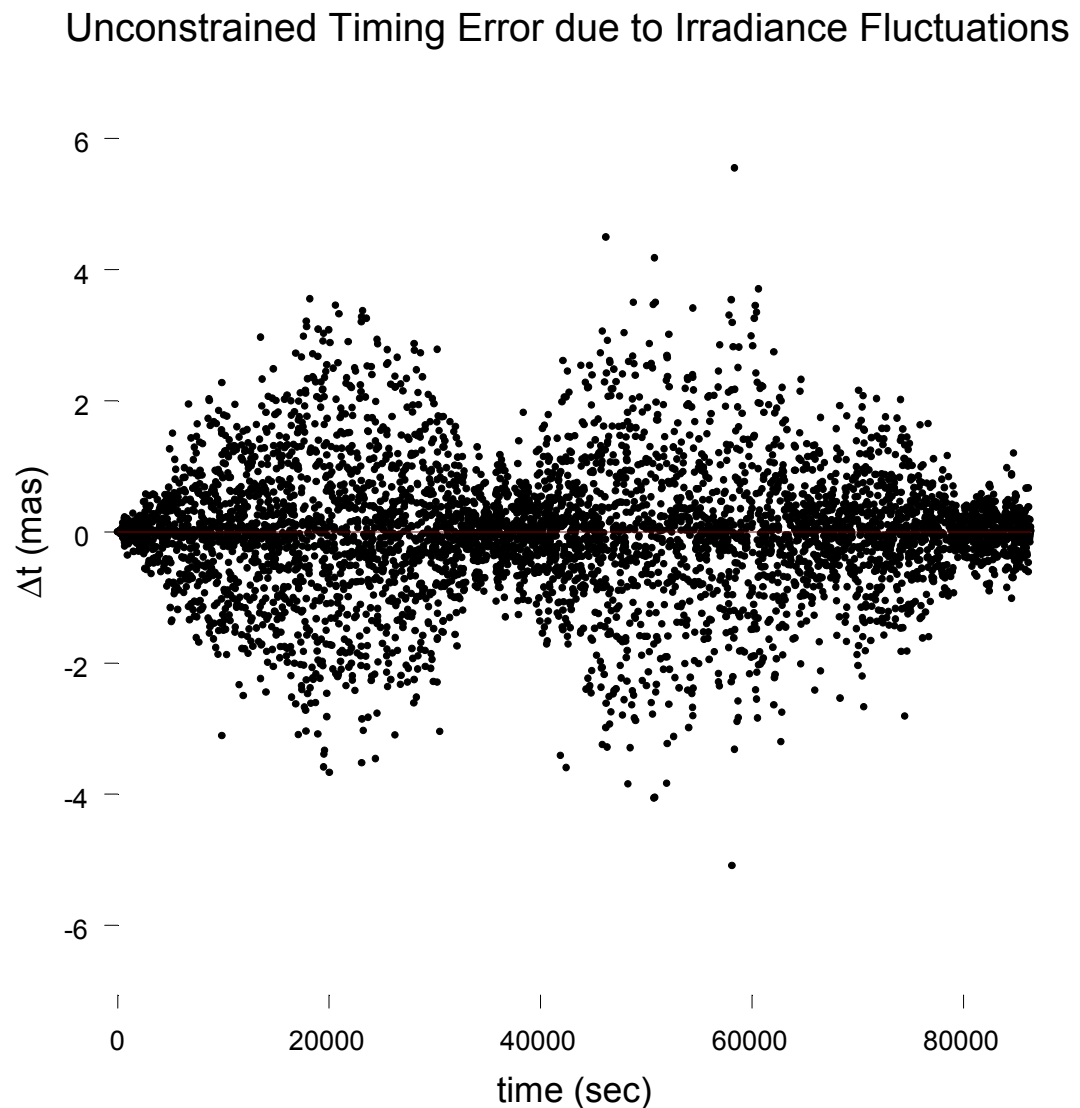


## Simulated Star Transit Observations (continued)

---

► Single-port (i.e., unconstrained) timing fluctuations due to irradiance fluctuations

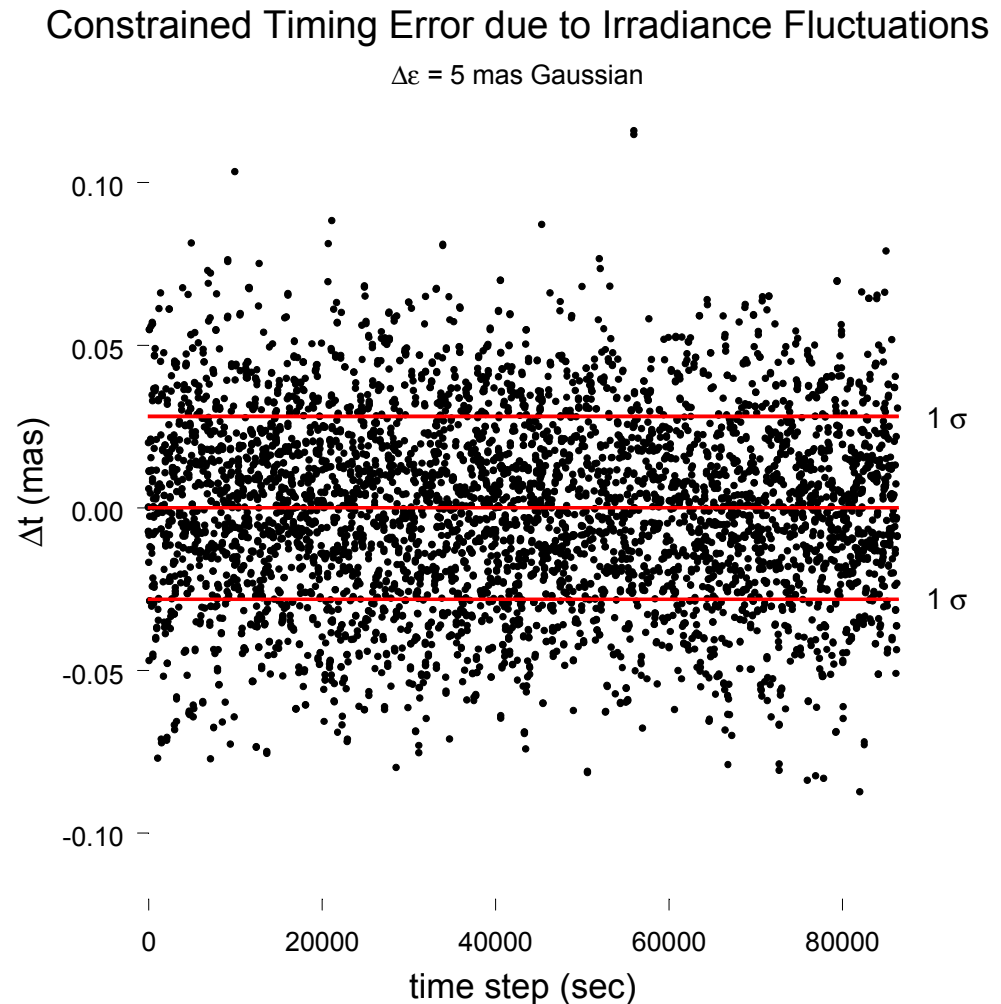
- $1\sigma$  errors  $\sim 1100 \mu\text{s}$
- Recall that our error budget is  $590 \mu\text{s}$



# Simulated Star Transit Observations (continued)

## ► Two-port (i.e., constrained) timing fluctuations

- field rotation attitude uncertainty constrained by cross-scan positions from the other viewport
- shown here:
  - assumed cross-scan uncertainty = 5 mas
  - timing errors constrained to 28  $\mu\text{s}$

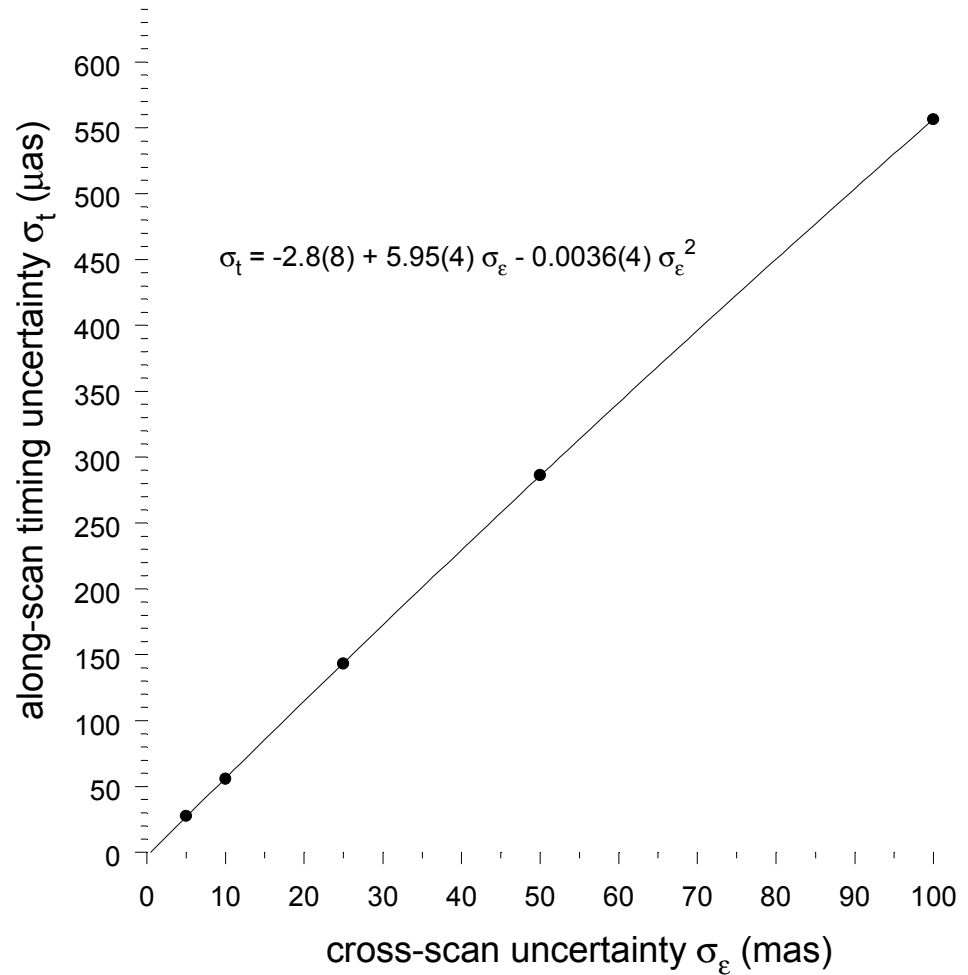




## Simulated Star Transit Observations (continued)

---

- Constrained timing errors as a function of cross-scan uncertainty

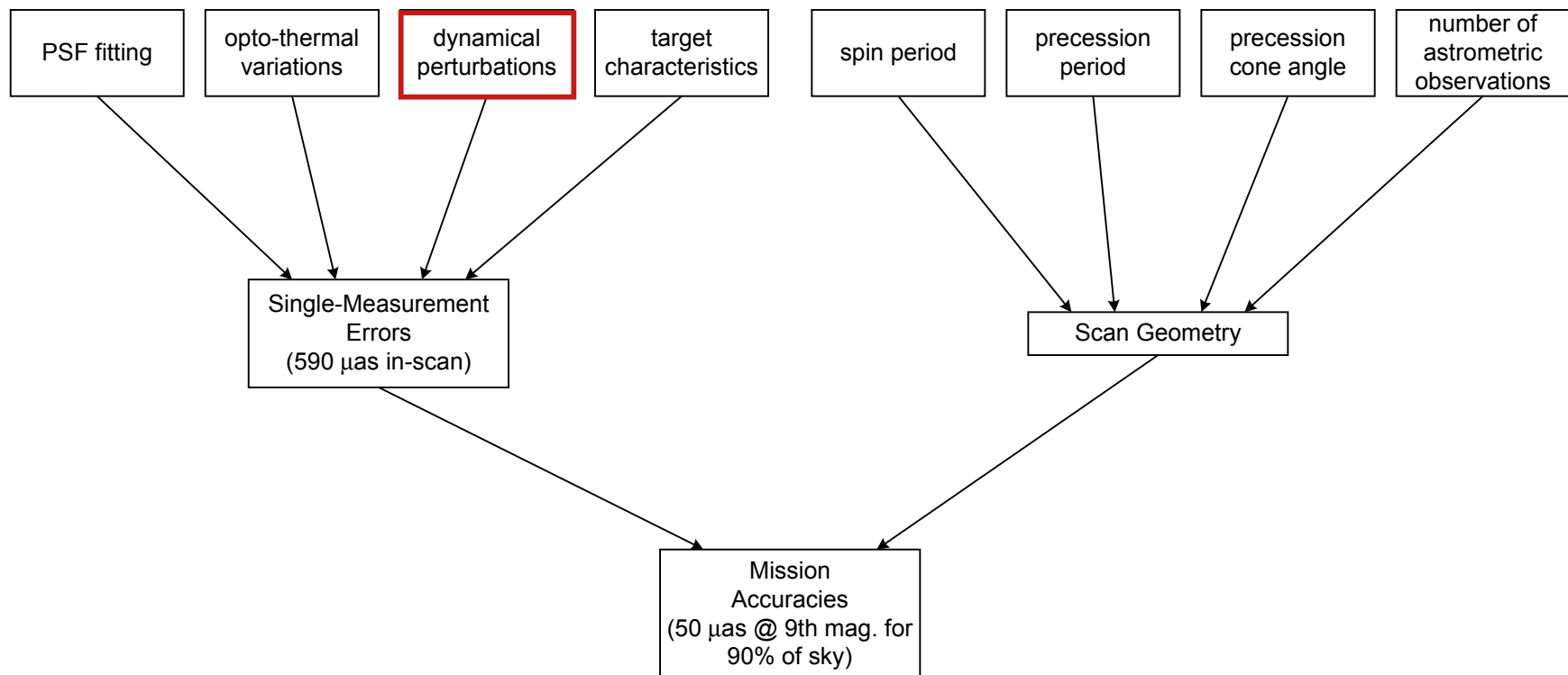


# Star motions at the focal plane

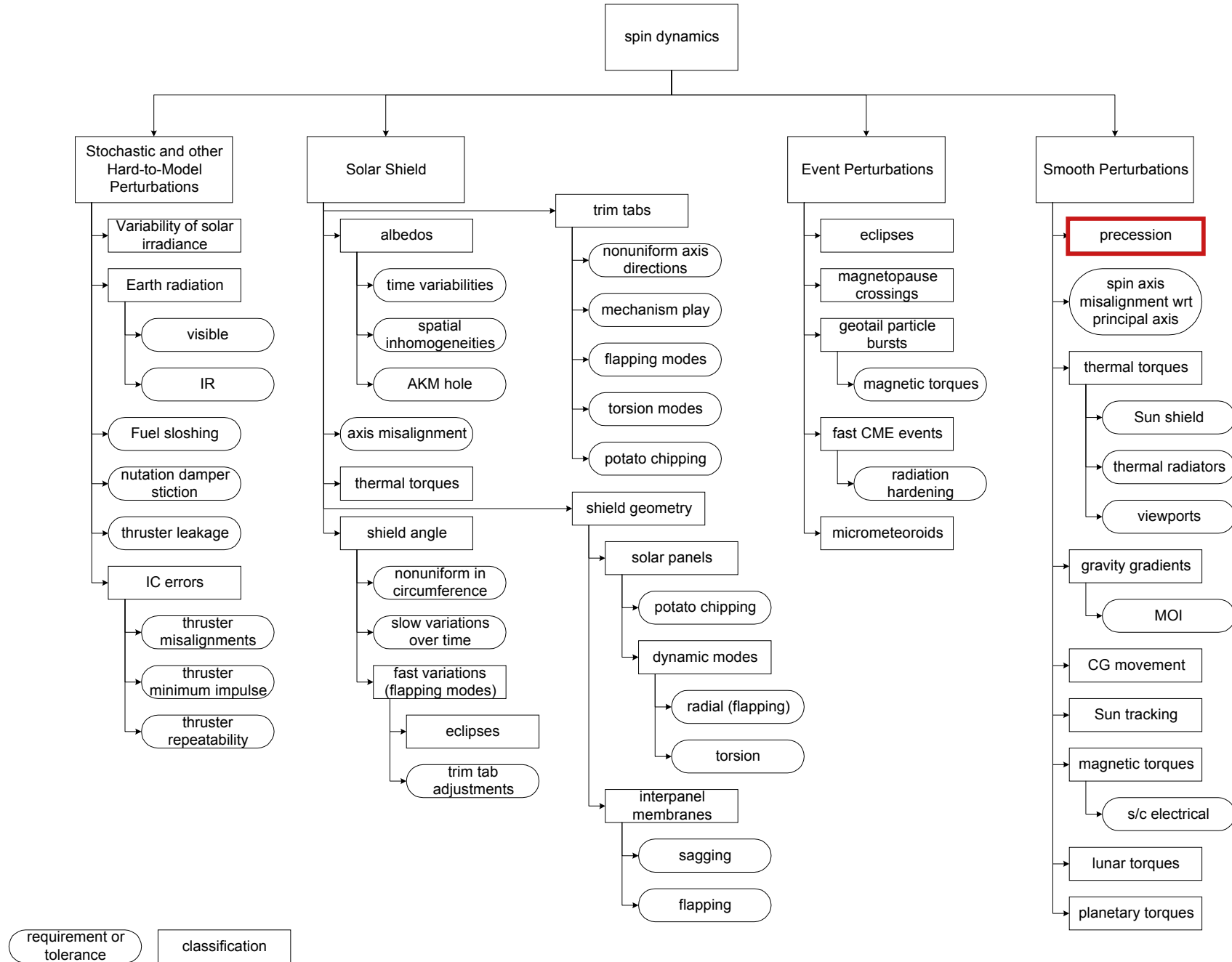
## What Determines Mission Accuracies? (cont.)

---

- ▶ nitty-gritties contribute to single-measurement errors ("local")
- ▶ observation density and scan angle distributions determined by scan geometry ("global")



# What Determines Mission Accuracies? (cont.)



# Focal Plane Motions

---

- ▶ The detailed path of a star across the FAME focal plane can be broken down into components (in order of magnitude):

## 1. Unperturbed spin about the symmetry axis

- period = 40 minutes
- results in straight-line motion across the long dimension of the CCDs

## 2. Unperturbed precession of the spin axis about the nominal Sun direction

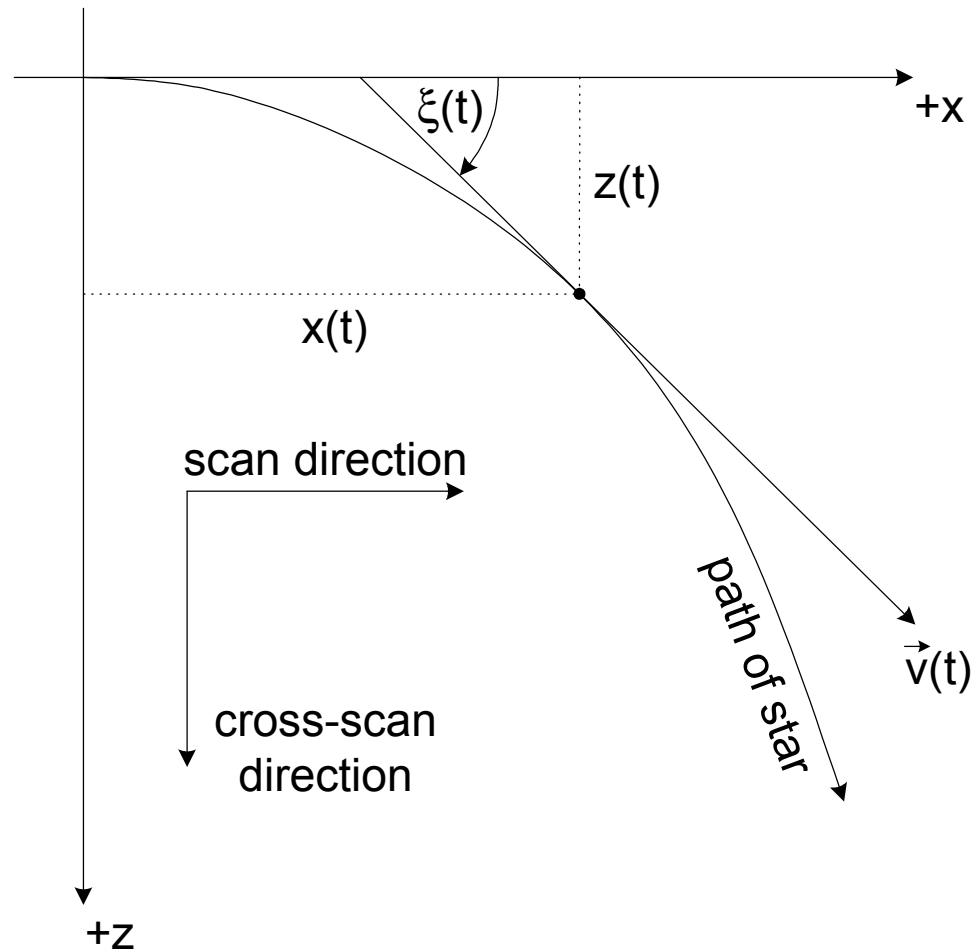
- period = 20 days
- causes a first-order cross-scan drift with amplitude that varies with spin phase
  - higher-order effects, too

## 3. Dynamical perturbations

- largest are likely to be
  - gravity gradients
  - perturbations due to shield geometric asymmetries and surface material inhomogeneities
  - magnetic torques
- as we have seen: lots and lots, we hope all small enough to deal with

## Focal Plane Motions (*cont.*)

---



## Focal Plane Motions (cont.)

► Focal plane velocity field: 
$$\left\{ \begin{array}{l} \frac{d}{d\theta} \eta(\theta) = -1 - \varepsilon_s(\theta) + \varepsilon_r(\theta) \zeta(\theta) \\ \frac{d}{d\theta} \zeta(\theta) = \varepsilon_c(\theta) - \varepsilon_r(\theta) \eta(\theta) \end{array} \right\}$$
 scan velocity  
cross-scan velocity

where

$$\varepsilon_c(t) = \frac{\Omega_c(t)}{\Omega_\theta}, \varepsilon_s(t) = \frac{\Omega_s(t)}{\Omega_\theta}, \varepsilon_r(t) = \frac{\Omega_r(t)}{\Omega_\theta}, \vec{\Omega}_s(t) = \vec{\Omega}(t) \cdot \hat{z} - \vec{\Omega}_\theta \quad \zeta = \frac{z}{f}, \text{ and } \eta = \frac{y}{f}$$

subscripts "s" = scan, "c" = cross-scan, "r" = field rotation

► Third-order expansion about a point in time (spin phase  $\theta$ ):

$$\left\{ \begin{array}{l} \frac{d}{d\theta} \eta(\theta) = -\frac{1}{2} \left[ \frac{d^2}{d\theta^2} \varepsilon_s(\theta) \right] \Delta^2 + \left\{ \left[ \frac{d}{d\theta} \varepsilon_r(\theta) \right] \zeta_0 - \frac{d}{d\theta} \varepsilon_s(\theta) + \varepsilon_r(\theta) \varepsilon_c(\theta) \right\} \Delta + \varepsilon_r(\theta) \zeta_0 - \varepsilon_s(\theta) - 1 \\ \frac{d}{d\theta} \zeta(\theta) = \left[ \frac{1}{2} \frac{d^2}{d\theta^2} \varepsilon_c(\theta) + \frac{d}{d\theta} \varepsilon_r(\theta) \right] \Delta^2 + \left\{ -\left[ \frac{d}{d\theta} \varepsilon_r(\theta) \right] \eta_0 + \frac{d}{d\theta} \varepsilon_c(\theta) + \varepsilon_r(\theta) \varepsilon_s(\theta) + \varepsilon_r(\theta) \right\} \Delta - \varepsilon_r(\theta) \eta_0 + \varepsilon_c(\theta) \end{array} \right\}$$

where  $\Delta$  = small time interval (e.g., CCD crossing time)

➡ *Given any angular velocity vector perturbation, we can write down the corresponding focal plane motions to any desired order*

# Focal Plane Motions — Precession

---

► Body frame rotations due to precession: 
$$\begin{bmatrix} \Omega_r \\ \Omega_c \\ \Omega_s \end{bmatrix} = \begin{bmatrix} \Omega_\varphi \sin \psi \sin \theta \\ \Omega_\varphi \sin \psi \cos \theta \\ \Omega_\theta + \Omega_\varphi \cos \psi \end{bmatrix}$$

► Resulting focal plane velocity field:

$$\left\{ \begin{array}{l} \frac{d}{d\theta} \eta(\theta) = (\zeta \sin \psi \cos \theta + \varepsilon \sin^2 \psi \sin \theta \cos \theta) \varepsilon \Delta + (\zeta \sin \psi \sin \theta - \cos \psi) \varepsilon - 1 \\ \frac{d}{d\theta} \zeta(\theta) = \frac{1}{2} \varepsilon \Delta^2 \sin \psi \cos \theta + (\varepsilon \sin \psi \sin \theta \cos \psi - \eta \sin \psi \cos \theta) \varepsilon \Delta + (-\eta \sin \theta + \cos \theta) \varepsilon \sin \psi \end{array} \right\}$$

1st order:  $\left\{ \frac{d}{d\theta} \zeta(\theta) = \varepsilon \sin \psi \cos \theta, \frac{d}{d\theta} \eta(\theta) = -\varepsilon \cos \psi \right\}$

2nd order:  $\left\{ \frac{d}{d\theta} \eta(\theta) = \varepsilon \zeta \sin \psi \sin \theta, \frac{d}{d\theta} \zeta(\theta) = -\varepsilon \eta \sin \theta \sin \psi \right\}$

3rd order:  $\left\{ \begin{array}{l} \frac{d}{d\theta} \zeta(\theta) = \Delta \varepsilon \sin \psi \left( \varepsilon \sin \theta \cos \psi + \frac{1}{2} \Delta \cos \theta - \eta \cos \theta \right) \\ \frac{d}{d\theta} \eta(\theta) = \Delta \varepsilon (\zeta + \varepsilon \sin \psi \sin \theta) \sin \psi \cos \theta \end{array} \right\}$



# focal plane velocity field and drift angle animations

This presentation is available at  
<http://aa.usno.navy.mil/murison/talks/>